The FASEB Journal article fj.12-221598. Published online May 2, 2013.



# Activated $\alpha_2$-macroglobulin induces Müller glial cell migration by regulating MT1-MMP activity through LRP1

**Pablo F. Barcelona,[1] Javier R. Jaldín-Fincati,[1] María C. Sánchez,[2] and Gustavo A. Chiabrando[2]**

Centro de Investigaciones en Bioquímica Clínica e Inmunología–Consejo Nacional de Investigaciones Cientificas y Tecnicas (CIBICI-CONICET), Departamento de Bioquímica Clínica, Facultad de Ciencias Químicas, Universidad Nacional de Córdoba, Córdoba, Argentina

ABSTRACT **In retinal proliferative diseases, Müller glial cells (MGCs) acquire migratory abilities. However, the mechanisms that regulate this migration remain poorly understood. In addition, proliferative disorders associated with enhanced activities of matrix metalloprotease 2 (MMP-2) and MMP-9 also present increased levels of the protease inhibitor $\alpha_2$-macroglobulin ($\alpha_2$M) and its receptor, the low-density lipoprotein receptor-related protein 1 (LRP1). In the present work, we investigated whether the protease activated form of $\alpha_2$M, $\alpha_2$M*, and LRP1 are involved with the MGC migratory process. By performing wound-scratch migration and zymography assays, we demonstrated that $\alpha_2$M* induced cell migration and proMMP-2 activation in the human Müller glial cell line, MIO-M1. This induction was blocked when LRP1 and MT1-MMP were knocked down with siRNA techniques. Using fluorescence microscopy and biochemical procedures, we found that $\alpha_2$M* induced an increase in LRP1 and MT1-MMP accumulation in early endosomes, followed by endocytic recycling and intracellular distribution of MT1-MMP toward cellular protrusions. Moreover, Rab11-dominant negative mutant abrogated MT1-MMP recycling pathway, cell migration, and proMMP-2 activation induced by $\alpha_2$M*. In conclusion, $\alpha_2$M*, through its receptor LRP1, induces cellular migration of Müller glial cells by a mechanism that involves MT1-MMP intracellular traffic to the plasma membrane by a Rab11-dependent recycling pathway.—Barcelona, P. F., Jaldín-Fincati, J. R., Sánchez, M. C., Chiabrando, G. A. Activated $\alpha_2$-macroglobulin induces Müller glial cell migration by regulating MT1-MMP activity through LRP1. *FASEB J.* 27, 000–000 (2013). www.fasebj.org**

*Key Words: endocytosis · intracellular traffic · proteases · retina · retinopathies*

$\alpha_2$-MACROGLOBULIN ($\alpha_2$M) is a plasma protease inhibitor with a broad specificity. Structurally, it is a tetrameric protein composed of two noncovalently associated dimers of disulfide-linked identical subunits (~180 kDa). $\alpha_2$M is characterized by a proteolysis-sensitive bait sequence and an internal β-cysteinyl-γ-glutamyl thiol ester bond per subunit. The bait region is susceptible to cleavage by proteinases, while the thiol ester bonds are a target to nucleophilic attack by monoamines (1). Consequently, $\alpha_2$M undergoes a conformational change and thus becomes an activated form, known as $\alpha_2$M*. This activated form specifically binds to the cell surface receptor low-density lipoprotein (LDL) receptor-related protein 1 (LRP1), a member of the LDL receptor gene family. However, $\alpha_2$M* only recognizes LRP1 among the LDL receptor members (2). The $\alpha_2$M-proteinase complex is internalized by LRP1 through clathrin-dependent endocytosis and degraded in lysosomes (3). In addition, binding of $\alpha_2$M* to LRP1 activates different intracellular signaling pathways, including ERK/MAPK, Akt, and NF-κB in Müller glial cells (MGCs), Schwann cells, and macrophages (4–7).

Abbreviations: $\alpha_2$M, α2-macroglobulin; $\alpha_2$M*, activated α2-macroglobulin; BrdU, 5-bromo-2′-deoxyuridine; ECM, extracellular matrix; FGF-2, fibroblast growth factor 2; GFAP, glial fibrillary acidic protein; GFP, green fluorescent protein; GST, glutathione *S*-transferase; LDL, low-density lipoprotein; LRP1, low-density lipoprotein receptor-related protein 1; MGC, Müller glial cell; MT1-MMP, membrane type I–matrix metalloprotease; MMP, matrix metalloprotease; NGF, nerve growth factor; PDGFRβ, platelet-derived growth factor receptor β; PDR, proliferative diabetic retinopathy; PKCα, protein kinase Cα; PVR, proliferative vitreoretinopathy; Rab, Ras-associated binding protein; RAP, receptor-associated protein; RFP, red fluorescent protein; siRNA, small interfering RNA; shRNA, small hairpin RNA; uPAR, urokinase-plasminogen activator receptor

[1] These authors contributed equally to this work.

[2] Correspondence: G.A.C., Centro de Investigaciones en Bioquímica Clínica e Inmunología–Consejo Nacional de Investigaciones Cientificas y Tecnicas (CIBICI-CONICET), Departamento de Bioquímica Clínica, Facultad de Ciencias Químicas, Universidad Nacional de Córdoba, Haya de la Torre y Medina Allende, Ciudad Universitaria, (5000) Córdoba, Argentina. E-mail: G.A.C., gustavo@fcq.unc.edu.ar; M.C.S., csanchez@fcq.unc.edu.ar

doi: 10.1096/fj.12-221598

This article includes supplemental data. Please visit *http://www.fasebj.org* to obtain this information.

LRP1 is a cell surface glycoprotein synthesized as a precursor protein of 600 kDa. It is proteolytically cleaved by furin into two subunits: a large subunit of 515 kDa (LRP1-α), containing the extracellular binding domain, and one of 85 kDa (LRP1-β) comprising the membrane spanning and cytoplasmatic domains. These subunits are associated through noncovalent interactions (3). LRP1 is a typical scavenger receptor that interacts and internalizes many different ligands in addition to $\alpha_2$M*. However, these ligands do not compete with each other for binding (3), with the exception of the receptor-associated protein (RAP). RAP binds to and blocks the binding of all known ligands to the receptor. After receptor-mediated endocytosis, certain ligands follow a lysosomal degradation pathway, such as $\alpha_2$M* and RAP (3), whereas others, such as apolipoprotein E (ApoE), are resecreted following a nondegradation pathway (8). However, regardless of the ligand interacting with LRP1, this receptor is internalized and accumulated mainly in the early endosomes (3). Noteworthy, endocytosis and intracellular trafficking of LRP1 seem to play a key role in the regulation of other plasma membrane receptors, such as the platelet-derived growth factor receptor β (PDGFRβ) and urokinase-plasminogen activator receptor (uPAR), thus controlling the cellular migration of different normal and malignant cells (9, 10).

In previous studies, we have demonstrated that increased expression of $\alpha_2$M and LRP1 was associated with an enhanced activity of matrix metalloprotease 2 (MMP-2) and MMP-9 in retinas of rats with ischemia-induced neovascularization. We also found that LRP1 was highly expressed in MGCs (11). Furthermore, $\alpha_2$M and LRP1 were increased in the vitreous and in retinas of human subjects with proliferative diabetic retinopathy (PDR), sickle cell retinopathy, and proliferative vitreoretinopathy (PVR) (12–14). However, the function of these two proteins in the aforementioned ischemic pathologies is not well established. The up-regulation of glial fibrillary acidic protein (GFAP) in MGCs is an early event under retinal stress conditions known as gliosis. Retinal ischemia-hypoxia, experimental glaucoma, and retinal detachment, major causes of severe visual loss, increase gene and protein expression of GFAP in MGCs (15–19). Interestingly, we have recently demonstrated that $\alpha_2$M* induced GFAP expression *via* LRP1 in the human Müller glial cell line MIO-M1, which seems to indicate that both proteins are involved in MGC activation during ischemic proliferative diseases (7).

In the retina, MGCs stabilize the complex retinal architecture, provide structural support to retinal neurons and blood vessels, and prevent aberrant photoreceptor migration into the subretinal space (20). It is well recognized that MGCs undergo functional and phenotypic changes in PVR and PDR, which involve cellular hypertrophy, process extension, migration, and proliferation, followed by extracellular matrix (ECM) remodeling (21, 22). Similar changes have occurred in animal models of retinal proliferation, in which intravitreal injections of inflammatory mediators caused rapid MGC migration and proliferation, followed by the formation of gliotic adhesions (23, 24). Both MMP-2 and MMP-9 have been involved in the development of PVR and PDR, suggesting that these MMPs may also facilitate MGC migration in the retina (22, 25).

Several MMPs, principally MMP-9, MMP-2, and membrane type 1-MMP (MT1-MMP), are involved in the cellular migration of normal and malignant cells (26). However, unlike MMP-9, which is primarily up-regulated at the transcriptional level, MMP-2 is constitutively expressed and secreted in a latent form (proMMP-2). The activation of proMMP-2 takes place at the cell surface and requires the participation of the active form of MT1-MMP (27), which is itself expressed in a latent form and intracellularly processed to its active form by furin (28). The activity of MT1-MMP at the cell surface level depends on its intracellular trafficking to the plasma membrane, which occurs through endocytic recycling and exocytic routes (29, 30). Given that $\alpha_2$M* and LRP1, in association with an enhanced activity of MMPs and ECM remodeling, seem to play active roles in ischemic proliferative retinopathies, we hypothesize that the binding of $\alpha_2$M* to LRP1 induces MGC migration. Thus, in the present work, we investigated the role of $\alpha_2$M*, LRP1, and MT1-MMP activity on MGC migration.

## MATERIALS AND METHODS

### Cell cultures and reagents

A spontaneously immortalized human Müller cell line (MIO-M1; ref. 31) was kindly provided by Dr. G. Astrid Limb (University College London, Institute of Ophthalmology and Moorfields Eye Hospital, London, UK). Cells were mantained in DMEM-high glucose (4.5 mg/ml) stabilized with 2 mM L-glutamine (GlutaMAX; Invitrogen, Buenos Aires, Argentina) and supplemented with 110 mg/ml sodium pyruvate, 10% (v/v) FCS, and 100 U/ml penicillin/streptomycin (Invitrogen), at 37°C with 5% $CO_2$. Then, $\alpha_2$M was purified from human plasma following a procedure previously reported (32), and $\alpha_2$M* was generated by incubating $\alpha_2$M with 200 mM methylamine–HCl for 6 h at pH 8.2, as described previously (33). An expression construct, encoding RAP as a glutathione *S*-transferase (GST) fusion protein (GST-RAP), was provided by Dr. Guojum Bu (Washington University, St. Louis, MO, USA), and GST-RAP was expressed and purified as reported before (34) and used without further modifications. In this work, 400 nM GST-RAP was used to inhibit the binding of $\alpha_2$M* to LRP1, whereas we previously demonstrated that the use of GST (400 mM) alone has no inhibitory effects (35). Immunoblots were performed with the following monoclonal antibodies: MT1-MMP antibody and LRP1 β-subunit antibody (clone 5A6), both from Calbiochem (Merck KGaA, Darmstadt, Germany). Human fibroblast growth factor 2 (FGF-2; code SRP2092) was purchased from Sigma-Aldrich (St. Louis, MO, USA).

### Transfection procedures

Wild-type MT1-MMP fused to green fluorescent protein (MT1-MMP-GFP) and cloned in a pEGFP-1 plasmid was

kindly provided by Dr. Jian Cao (Stony Brook University, Stony Brook, NY, USA; ref. 36). GFP and red fluorescent protein (RFP) wild-type Ras-associated binding protein 11 (Rab11) plasmids (GFP-wt-Rab11 and RFP-wt-Rab11) and dominant-negative mutant of Rab11 plasmid (GFP-Rab11S25N) were kindly donated by Dr. María Isabel Colombo (Instituto de Histología y Embriología, Facultad de Ciencias Médicas, Universidad Nacional de Cuyo–Consejo Nacional de Investigaciones Cientificas y Tecnicas, Mendoza, Argentina). MIO-M1 cells ($4\times10^5$ cells/well) were cultured in 6-well plates and transiently transfected with 2 μg of either pGFP/pRFP empty vectors or pGFP/pRFP plasmids expressing target GFP/RFP fusion proteins for 6 h, using Lipofectamine 2000 (Invitrogen), according to the manufacturer's instructions. Then, the cells were washed and incubated for 18 h in DMEM-high glucose at 37°C with 5% $CO_2$.

### Small interfering RNA (siRNA)- and small hairpin RNA (shRNA)-mediated gene silencing of LRP1 and MT1-MMP

To inhibit LRP1 expression, MIO-M1 cells were transiently transfected with annealed siRNA (siRNA-LRP1), which had been synthesized by Ambion (Austin, TX, USA), according to previously published LRP1 target sequences (37). siRNA-LRP1 was a 15-mer (5′-CGGCGGGGTCAGCAT-3′) oligonucleotide complementary to nt 466 to 481 of LRP1 mRNA. A random siRNA was used as a negative control (Ambion AM 4636) in cellular transfections. In addition, the LRP1 silencing was also carried out with shRNA directed against the 3′-untranslated region of the wild-type human LRP mRNA (5′-GAACTCTCCCTTCCCAGAATTAGCTAATTCTGGGAAG-GGAGAGTTCTT-3′ pos. 14493–14518 of the endogenous human LRP mRNA; noncoding 3′-UTR; accession no. X13916), which was kindly provided by Dr. Alexander Laatsch (University Medical Center Hamburg-Eppendorf, Hamburg, Germany). To inhibit MT1-MMP expression, MIO-M1 cells were transiently transfected with annealed siRNA (siRNA-MT1-MMP), which had been synthesized by Ambion transfection (siRNA ID s8879). siRNA-MT1-MMP was a 21-mer (5′-GCAACAUAAUGAAAUCACACU-3′). Procedures were performed using the transfection agent siPORT NeoFX siRNA (Ambion) for siRNA and Lipofectamine 2000 (Invitrogen) for shRNA, according to the manufacturer's instructions. In all cases, experiments were performed 24 h after transfection. To test the level of protein silencing, LRP1 was evaluated by Western blot analysis in transfected cells.

### Cell migration assays

Cell migration activities were examined by a 2-dimensional wound-scratch assay in 6-well plates coated with collagen type I (10 $\mu g/cm^2$; Sigma-Aldrich). MIO-M1 cells ($5\times10^5$ cells/well) were cultured for 48 h at 37°C in DMEM-high glucose containing 10% FCS and 2 mM L-glutamine with 5% $CO_2$, followed by overnight serum depletion. In each well, a straight lesion was created in the center of the MIO-M1 cell monolayer with a sterile 10-μl pipette tip. This technique produced a consistent wound devoid of cells, ~35 mm long × 400 μm wide. Wells were then rinsed twice with serum-free medium to remove any cell debris, and 2 ml of DMEM-high glucose without red phenol was added. Cells were treated with 60 nM $\alpha_2$M* for different times. To block $\alpha_2$M*-LRP1 binding, cells were previously treated with 400 nM GST-RAP for 30 min. At 24 h after siRNA-MT1-MMP, siRNA-LRP1, or shRNA-LRP1 transfection, the MIO-M1 cells were plated as indicated above. Similar experiments were carried out with MIO-M1 cells transfected with GFP-wt-Rab11 and GFP-Rab11S25N plasmids. Cellular migration was measured following the procedure described previously (38). Briefly, at selected times (0 and 12 h), 3 random images of the wound per condition were acquired using a charge-coupled device (CCD) camera (Nikon) on a bright-field microscope (Nikon TU-2000 inverted microscope; Nikon, Tokyo, Japan) with a ×10 objective (0.3 NA). Each image defined an average area of the wound equivalent to $5 \times 10^5 \pm 1 \times 10^4$ $\mu m^2$ recorded to $t = 0$ h. Cells invading this area were counted to $t = 12$ h, and results were expressed as cells per area. For cell proliferation assays, MIO-M1 cells were cultured as indicated above. Then, cells were treated either with $\alpha_2$M* (60 nM) or FCS (10%) as a positive control, followed by the addition of 10 μM 5-bromo-2′-deoxyuridine (BrdU; Invitrogen). After a 24-h incubation period, cells were fixed, permeabilized, and treated with 1 M HCl for 30 min at room temperature. Then, cells were rinsed twice with 0.1 M boric acid/borate buffer (pH 8.5) and PBS, and incubated with an antibody anti-BrdU (Sigma-Aldrich). The reaction was revealed with the secondary antibody anti-IgG conjugated with Alexa Fluor 594 (Invitrogen).

### Gelatin zymography assays

To examine the gelatinolytic activity of MMPs, MIO-M1 cells ($5\times10^5$ cells/well) were cultured at 37°C for 24 h in DMEM-high glucose containing 10% FCS and 2 mM L-glutamine with 5% $CO_2$. Cells were rinsed twice with serum-free medium, and 2 ml of DMEM-high glucose was added. Cells were stimulated with 60 nM $\alpha_2$M* for different times, after which the cell culture supernatants were collected and concentrated using the Centricon-10 system (Millipore, Toronto, ON, Canada). Aliquots of concentrated medium containing 50 μg of total protein were resolved on a 7.5% SDS-PAGE/1.5% gelatin (39). Then, gels were rinsed for 1 h with 2.5% Triton X-100 and 40 nM Tris-HCl (pH 7.6), before being incubated at 37°C for 48 h in enzyme buffer (50 mM Tris HCl, 0.2 M NaCl, and 5 mM $CaCl_2$, pH 7.6). To visualize proteolytic MMP activity, gels were fixed in 45% methanol/10% acetic acid, and then stained for 30 min in 0.125% Coomassie blue R-250.

### Epifluorescence and confocal microscopy

To visualize the MT1-MMP cellular localization, MIO-M1 cells transfected or nontransfected with GFP-MT1-MMP were grown on glass coverslips coated with collagen type I (10 $\mu g/cm^2$) before being stimulated or not with $\alpha_2$M* (60 nM). These cells were washed with PBS, fixed with 4% paraformaldehyde, and incubated with a quenching solution (50 mM glycine). After this, transfected and nontransfected cells were permeabilized with 0.1% (v/v) Triton X-100, and blocked with 2% BSA. In contrast, cells that had not been transfected were incubated with an anti-MT1-MMP antibody followed by incubation with a secondary antibody conjugated with Alexa Fluor 488 (Invitrogen, Buenos Aires, Argentina). Finally, cells were washed with PBS and mounted on glass slides with Mowiol 4–88 reagent from Calbiochem (Merck KGaA, Darmstadt, Germany). Fluorescent images were obtained using a CCD camera (Nikon) in an epifluorescence microscope (Nikon TU-2000) and were processed with ImageJ software (Rasband, W. S., U. S. National Institutes of Health, Bethesda, MD, USA, http://imagej.nih.gov/ij/). To evaluate the colocalization between MT1-MMP and LRP1 by immunofluorescence microscopy, the MIO-M1 cells were transfected with MT1-MMP-GFP and grown on coverslips coated with collagen type I (10 $\mu g/cm^2$). After stimulus with 60 nM $\alpha_2$M* for different times, coverslips were processed as described above and then incubated with a primary LRP1 β-subunit antibody (clone 5A6). Next, coverslips were incubated with a secondary

antibody raised in goat against mouse IgG conjugated with Alexa Fluor 594 (Molecular Probes, Eugene, OR, USA), and fluorescent images were obtained with an Olympus FluoView FV300 confocal laser scanning biological microscope (Olympus, New York, NY, USA). Whole cells were scanned, and optical sections were gathered in 0.25-μm steps perpendicular to the *z* axis. Finally images were processed using FV10-ASW Viewer 3.1 (Olympus) and ImageJ software.

To examine the colocalization of MT1-MMP and LRP1 in early endosomes by confocal microscopy, the MIO-M1 cells were transfected with GFP-MT1-MMP and processed as indicated above. After being stimulated with $\alpha_2$M* for different times, coverslips were incubated with a primary rabbit anti-EEA1 antibody (Abcam, Cambridge, MA, USA) and a mouse anti-LRP1 β-subunit antibody (clone 5A6). Then, coverslips were incubated with secondary antibodies raised in goat against rabbit and mouse IgG conjugated with Alexa Fluor 647 and 594, respectively. Fluorescent images were obtained with an Olympus FluoView FV1000 confocal laser scanning biological microscope (Olympus), whole cells were scanned, and optical sections were gathered in 0.25-μm steps perpendicular to the *z* axis. Finally, images were processed as indicated above. To analyze the colocalization between MT1-MMP and LRP1 in recycling compartments, MIO-M1 cells transfected with RFP-wt-Rab11 and GFP-MT1-MMP were used. LRP1 analyses were carried out as described above. To block the Rab11-recycling pathway, MIO-M1 cells were transfected with GFP-Rab11S25N, and MT1-MMP was immunodetected as indicated above.

### Immunoprecipitation assays

MIO-M1 cells ($1.2\times10^6$ cells/60-mm plate) were cultured at 37°C for 24 h in DMEM-high glucose containing 10% FCS and 2 mM L-glutamine with 5% $CO_2$. Then, cells were treated with 60 nM $\alpha_2$M* for different times, and cell protein extracts were prepared using nondenaturing lysis buffer (20 mM Tris-HCl, 137 mM NaCl, 10% glycerol, 1% Triton-X100, and 2 mM EDTA, pH 8.0) containing 1 mM phenylmethylsulfonyl fluoride (PMSF) and protease inhibitor cocktails (Sigma-Aldrich). Protein extracts were incubated overnight at 4°C with either mouse anti-MT1-MMP monoclonal antibody, mouse anti-LRP1 α-subunit monoclonal antibody (Clon MCA1965; AbD Serotec, Oxford, UK), or mouse nonimmune IgG as the IP control (code ab81032; Abcam, Cambridge, MA, USA) (1 μg/200 μg of total proteins) cross-linked with 50 mM dimethyl pimelimidate dihydrochloride (DMP) to protein G-Sepharose magnetic beads following the manufacturer's procedure (protein G Mag Sepharose; GE Healthcare Bio-Sciences AB, Uppsala, Sweden).

### Biotin-labeling cell surface protein assay

MIO-M1 cells ($1.2\times10^6$ cells/60-mm plate) were cultured at 37°C for 24 h in DMEM-high glucose containing 10% FCS and 2 mM L-glutamine with 5% $CO_2$. Then, cells were treated with 60 nM $\alpha_2$M* for different times. To detect the cell surface level of MT1-MMP, a biotin-labeling protein assay (Thermo Scientific, Rockford, IL, USA) was used following the manufacturer's procedure. After that, the biotin MT1-MMP was immunoprecipitated using the same procedure as described previously. Similar experiments were carried out with MIO-M1 cells transfected with GFP-wt-Rab11 and GFP-Rab11S25N plasmids. Equal amounts of eluted proteins were resolved on SDS-PAGE and blotted with HRP-conjugated streptavidin (Thermo Scientific) before being revealed by a chemioluminiscense kit as indicated above. To control the amount of transfected GFP-fusion proteins, immunoblots were performed using a polyclonal rabbit anti-GFP antibody (Abcam).

### Statistical treatment of data

For the densitometric quantifications and cellular migration assays, results are expressed as mean ± SEM of independent experiments, and one-way ANOVA was used for comparisons. Differences from the control were considered significant at $P < 0.05$. For microscope quantifications of the level of colocalization, a JACoP plug-in from ImageJ software was used (40). At least 50 cells/condition were analyzed. Then, the averages of the vesicle percentages containing both proteins were calculated from the Manders' coefficients and compared using the Student's *t* test. Values of $P < 0.05$ were considered significant.

## RESULTS

### $\alpha_2$M* induces MIO-M1 cell migration through LRP1

It is well known that the MIO-M1 cell line retains phenotypic and functional characteristics of primary isolated MGCs in culture (31) and constitutively expresses LRP1 (7). To investigate the effect of $\alpha_2$M* in MGC migration, we used a two-dimensional wound-scratch assay where MIO-M1 cells were cultured in collagen type I-coated plates. **Figure 1*A*** shows representative wound-scratch assays of MIO-M1 cells cultured in the absence or presence of $\alpha_2$M*. The quantitative analysis revealed that $\alpha_2$M* significantly increased the number of cells migrating to the lesion site after 12 h of stimulus when compared to nonstimulated cells (Fig. 1*B*). On the other hand, by using the BrdU assay, we demonstrated that 24 h of $\alpha_2$M* stimulus did not induce proliferation on MIO-M1 cells (Fig. 1*C*). Next, to examine whether $\alpha_2$M*-induced cell migration was mediated by LRP1, MIO-M1 cells were pretreated with GST-RAP (400 nM) for 1 h to inhibit $\alpha_2$M* binding to LRP1 (3, 35). Figure 1*B* shows that GST-RAP blocked the effect of $\alpha_2$M* on cell migration, indicating that LRP1 was required. Finally, to evaluate the specific role of LRP1 in the cellular migration induced by $\alpha_2$M*, the receptor expression was knocked down by two different RNA-silencing techniques: vector-based shRNA and siRNA for LRP1. Figure 1*D* shows that both techniques significantly decreased the protein level of LRP1 (~70 and ~80% for shRNA and siRNA, respectively). This protein suppression was sustained for ≥72 h after transfection with both RNA-silencing techniques (data not shown). Figure 1*E* demonstrates that LRP1 knockdown in MIO-M1 cells significantly decreased $\alpha_2$M*-induced cellular migration. In contrast, LRP1 reduction in MIO-M1 cells did not interfere with the cellular migration induced by the fibroblast growth factor 2 (FGF-2; ref. 41). Thus, we conclude that $\alpha_2$M*-promoted MIO-M1 cell migration is mediated by LRP1.

### $\alpha_2$M* induces proMMP-2 activation through LRP1

Retinal MGCs can regulate the expression and activity of MMP-2 and MMP-9, which may be implicated in

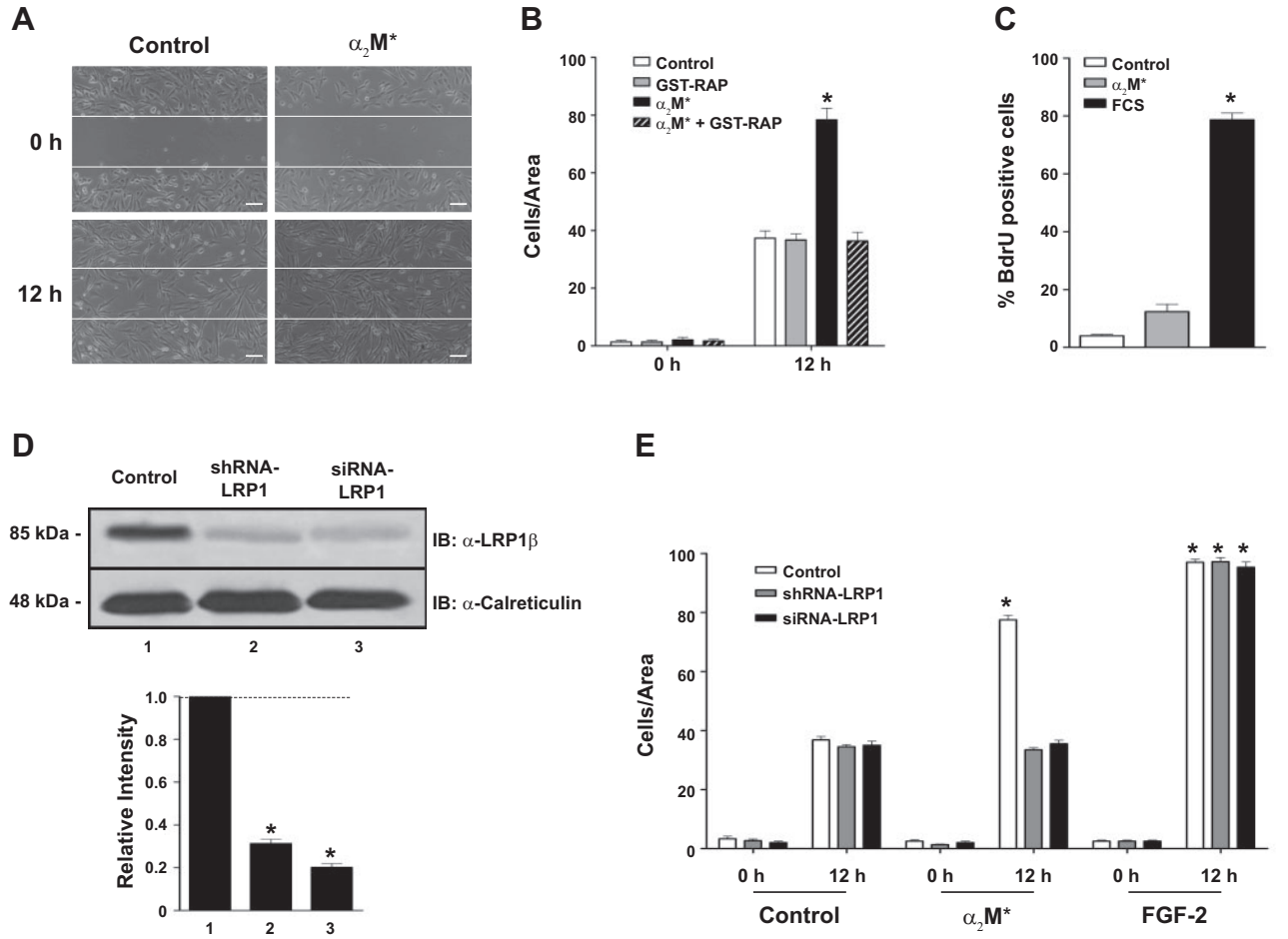


**Figure 1.** $\alpha_2$M* induces MIO-M1 cell migration through LRP1. Cells were cultured for 12 h in serum-free DMEM, in the absence or presence of $\alpha_2$M* (60 nM). *A*) Wound-scratch assay of MIO-M1 cells cultured in plates coated with collagen type-I. $\alpha_2$M* induced a significant migration of MIO-M1 cells during 12 h of stimulus with respect to control. Scale bars = 100 μm. *B*) Mean values of the cell number invading the area of the wound (cells/area) in the absence (control) or presence of $\alpha_2$M* (60 nM). For blocking the $\alpha_2$M* binding to LRP1, cells were pretreated with GST-RAP (400 nM) for 30 min and then stimulated with $\alpha_2$M* (60 nM) for 12 h. *C*) Cell proliferation assay using the BrdU technique for 24 h of $\alpha_2$M* (60 nM) stimulation. $\alpha_2$M* did not induce cellular proliferation of MIO-M1 cells respect to control. FCS (10%) was used as a positive control of cell proliferation. *D*) Immunoblotting (IB) for LRP1 (α-LRP1β, monoclonal antibody anti-LRP1 β subunit) of whole-cell lysates of MIO-M1 cells transfected with shRNA-LRP1 or siRNA-LRP1. Densitometric analysis shows that a significant reduction of the LRP1 level in MIO-M1 cells was produced with both protein-silencing techniques. Immunoblotting for calreticulin (α-calreticulin, monoclonal antibody anti-calreticulin), which was used as protein loading control. *E*) Mean values of the cell number invading the area of the wound (cells/area) for cells transfected with shRNA-LRP1 or siRNA-LRP1 and then stimulated with $\alpha_2$M* (60 nM) for 12 h. FGF-2 (10 ng/ml) was used as a positive control of the cellular migration in cells transfected with shRNA-LRP1 and siRNA-LRP1 with respect to siRNA-random transfected cells (control). Wound-scratch assay and RNA-silencing procedures are detailed in Material and Methods. Three independent experiments were performed in triplicate. Values are expressed as mean ± SEM. $^*P < 0.05$ *vs.* control.

cellular migration and extracellular matrix remodeling (22). Herein, we evaluated whether $\alpha_2$M* could affect the gelatinolytic activity of MIO-M1 cells. To determine the latent and active forms of MMP-2 and MMP-9, cells were incubated with $\alpha_2$M* for different times, and cell culture supernatants were analyzed by a gelatin zymography assay. **Figure 2*A*** shows that, after 1 h, $\alpha_2$M* induced proMMP2 activation, as evidenced by the presence of a gelatinolytic band with molecular weight lower than the latent form (68 kDa), which is compatible with its active form (either intermediate or active MMP-2). On the other hand, neither latent nor active forms of MMP-9 were detectable in cell culture supernatants of MIO-M1 cells stimulated or not with $\alpha_2$M* for 1 and 2 h (data not shown). Next, and to examine whether LRP1 was mediating $\alpha_2$M*-induced proMMP-2 activation, MIO-M1 cells were preincubated with GST-RAP, followed by the zymography assay. Figure 2*B* shows that GST-RAP abolished $\alpha_2$M*-induced proMMP-2 activation in MIO-M1 cells. In the same way, LRP1 knockdown blocked proMMP-2 activation induced by $\alpha_2$M* in MIO-M1 cells transfected with shRNA- or siRNA-LRP1 (Fig. 2*C*). Moreover, $\alpha_2$M*-induced proMMP-2 activation was inhibited in MIO-M1 cells where MT1-MMP had been knocked down (Fig. 2*D*). Interestingly, $\alpha_2$M*-induced cellular migration was also inhibited by

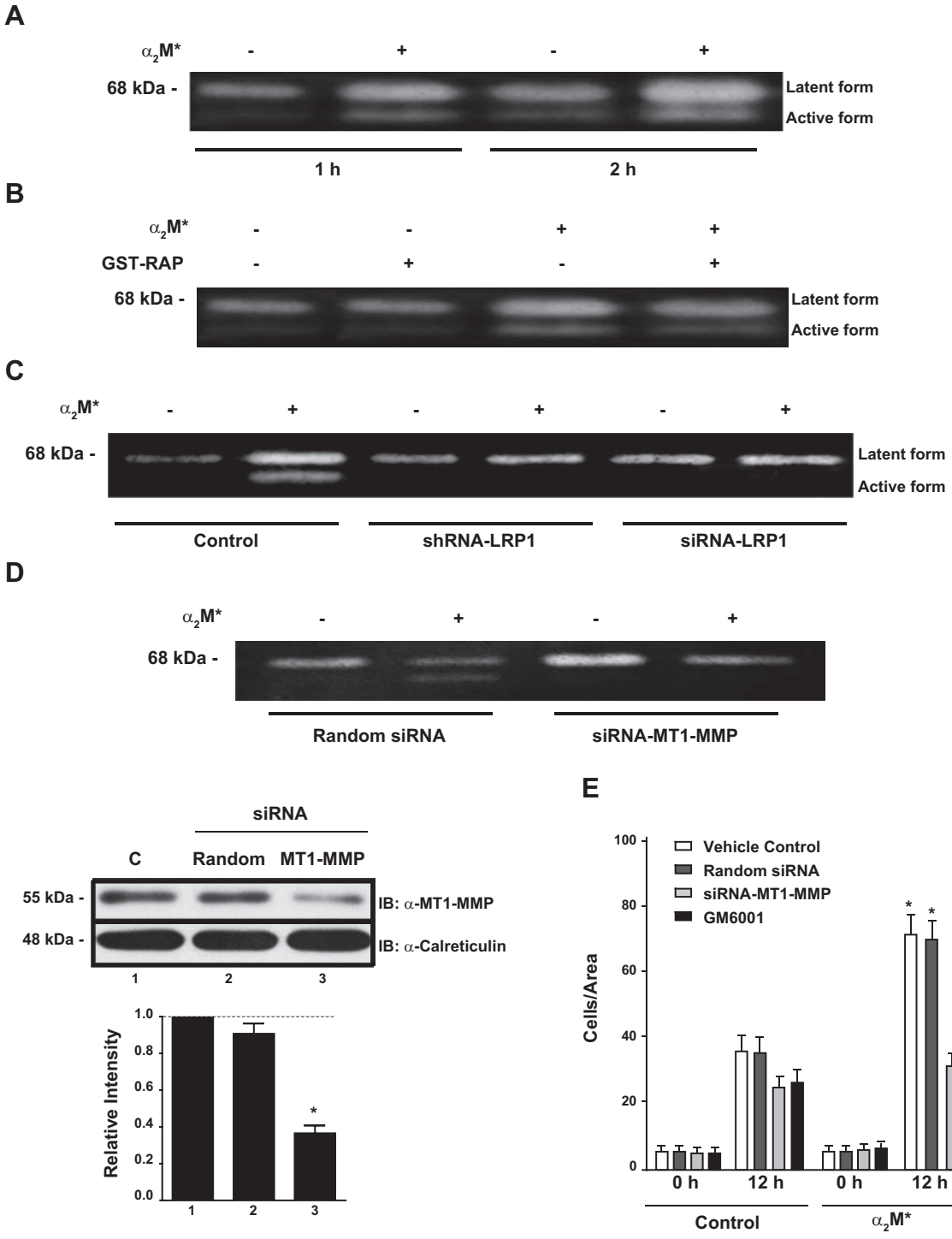


**Figure 2.** $\alpha_2$M* induced the proMMP-2 activation through LRP1. MIO-M1 cells were cultured in serum-free DMEM, in the absence or presence of $\alpha_2$M* (60 nM). *A*) Zymography assay of culture supernatants of MIO-M1 cells stimulated with $\alpha_2$M* for 1 or 2 h. $\alpha_2$M* induces proMMP-2 activation (Latent form) to either intermediate or active MMP-2 (Active form). The proMMP-2 molecular weight (68 kDa) is indicated. *B*) Zymography assay of culture supernatants of MIO-M1 cells pretreated with GST-RAP (400 nM) for 30 min and then stimulated with $\alpha_2$M* for 1 h. GST-RAP blocked $\alpha_2$M*-induced proMMP-2 activation to active MMP-2. *C*) Zymography assay of culture supernatants of MIO-M1 cells transfected with shRNA-LRP1 or siRNA-LRP1 and then stimulated with $\alpha_2$M* for 1 h. LRP1 knockdown inhibited $\alpha_2$M*-induced proMMP-2 activation. *D*) Zymography assay of culture supernatants of MIO-M1 cells transfected with siRNA-MT1-MMP or random siRNA and stimulated with $\alpha_2$M* for 1 h. MT1-MMP knock-down inhibited $\alpha_2$M*-induced proMMP-2 activation. Immunoblotting (IB) for MT1-MMP of MIO-M1 cells transfected with siRNA-MT1-MMP or random siRNA is showed. Calreticulin (α-calreticulin) was used as protein loading control. *E*) Wound-scratch assay of MIO-M1 cells cultured in plates coated with collagen type-I. Bar graph represents mean values of the cell number invading the area of the wound (cells/area) for cells transfected with siRNA-MT1-MMP or random siRNA and for cells pretreated with 20 μM GM6001 or serum-free DMEM (vehicle control) for 30 min and then stimulated with $\alpha_2$M* (60 nM) for 12 h. Three independent experiments were performed in triplicate. Values are expressed as mean ± SEM. *$P < 0.05$ *vs.* control.

siRNA-MT1-MMP and GM6001 MMP inhibitor, indicating that the cell motility is mediated by MT1-MMP and extracellular MMP activity (Fig. 2*E*). These results indicate that the $\alpha_2$M*-LRP1 interaction induced proMMP-2 activation through a molecular mechanism that requires MT1-MMP.

### $\alpha_2$M* regulates the cellular distribution of MT1-MMP

It is well established that proMMP-2 activation occurs at the plasma membrane (preferentially at the leading edge of motile cells) and is mediated by MT1-MMP and TIMP-2 (42). In addition, the subcellular localization and polarized distribution of active MT1-MMP at the cell surface are key events for cellular migration and proMMP-2 activation (26, 43). Considering our results reported above, we decided to investigate the effects of $\alpha_2$M* on the cellular distribution of MT1-MMP in MIO-M1 cells. In particular, the constitutive cell localization of MT1-MMP, in cells cultured in the presence of $\alpha_2$M* for 1 h, was explored using epifluorescence microscopy. **Figure 3** (top panels) shows a polarized distribution of MT1-MMP at the cellular protrusions in $\alpha_2$M*-stimulated MIO-M1 cells. Similar experiments were carried out in cells transiently transfected with a GFP-tagged wild-type MT1-MMP plasmid (GFP-MT1-MMP). We found that $\alpha_2$M* promoted the distribution of GFP-MT1-MMP toward the cellular protrusions of MIO-M1 cells cultured in the presence of $\alpha_2$M* (Fig. 3, bottom panels). The cellular redistribution of both constitutive MT1-MMP and transfected GFP-MT1-MMP induced by $\alpha_2$M* was abolished when the MIO-M1 cells were pretreated with 400 nM GST-RAP (Fig. 3), indicating that the effect of $\alpha_2$M* on MT1-MMP cell distribution was mediated by LRP1.

### $\alpha_2$M* induces MT1-MMP endocytic recycling

The activity of MT1-MMP at the cell surface level depends on its intracellular traffic to the plasma membrane, which occurs through at least the following two routes: *1*) an endocytic recycling route that is Rab11-dependent; and *2*) an exocytic route regulated by Rab8 (29, 30, 44). The endocytic recycling of MT1-MMP to the plasma membrane results from its continuous clathrin- and nonclathrin-dependent endocytosis, which are both routed to early and late endosomes before being recycled back to the plasma membrane (45). In con-

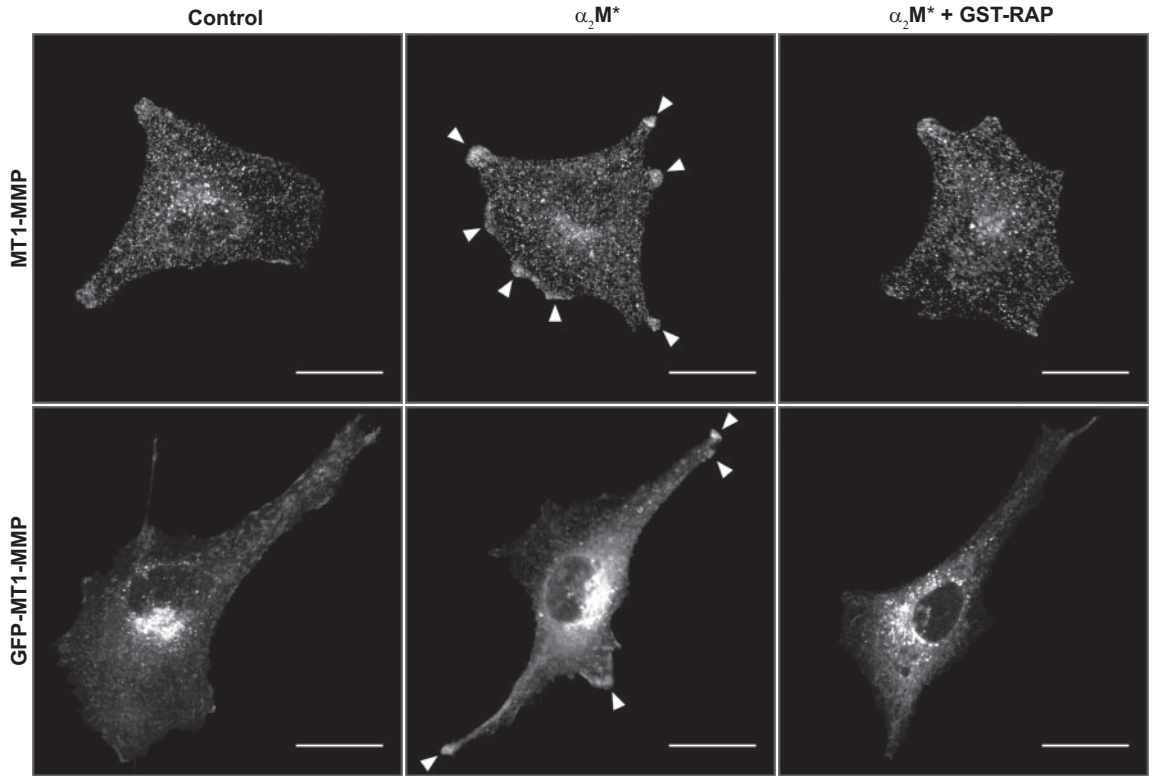


**Figure 3.** $\alpha_2$M* induced the intracellular distribution of MT1-MMP toward cellular protrusions. Top panels: epifluorescence microscopy of the MT1-MMP immunodetection using a specific monoclonal antibody in MIO-M1 cells cultured in glass coverslips coated with collagen type I and then treated with serum-free DMEM (control), $\alpha_2$M* (60 nM) for 1 h or pretreated with GST-RAP (400 nM) for 30 min and then stimulated with $\alpha_2$M* for 1 h. This panel shows that MT1-MMP is localized in cellular protrusions (arrowhead) with respect to MIO-M1 cells nonstimulated with $\alpha_2$M* (control), where MT1-MMP presents a diffuse cellular distribution. GST-RAP inhibits the $\alpha_2$M*-induced MT1-MMP localization in cellular protrusions. Bottom panels: epifluorescence microscopy of GFP-MT1-MMP-transfected MIO-M1 cells cultured and treated as indicated above. GFP-MT1-MMP is localized in cellular protrusions (arrowhead) of MIO-M1 cells that were stimulated with $\alpha_2$M* with respect to nonstimulated cells (control), this being also inhibited by GST-RAP. Scale bars = 10 μm. Details of epifluorescence microscopy and experiments are reported in Materials and Methods. All results are representative of 3 independent experiments.

trast, the exocytic route involves MT1-MMP mobilization from biosynthetic storage compartments, which is induced by cell-MEC contact (30). It has been suggested that both these routes are implicated in the control of MT1-MMP delivery to invadopodia, when cells need to respond in a fast and transient manner to soluble mitogenic factors (43). Thus, considering that $\alpha_2$M* *via* LRP1 can induce the intracellular distribution of MT1-MMP toward cellular protrusions, herein we evaluate using confocal microscopy the endocytosis and endocytic recycling pathways of MT1-MMP, in association with LRP1, in GFP-MT1-MMP transfected MIO-M1 cells treated with $\alpha_2$M*. **Figure 4** shows that $\alpha_2$M* (30 min) induced a significant increase of GFP-MT1-MMP/LRP1 colocalization (~60%) in perinuclear vesicles, when compared to nontreated MIO-M1 cells (~20%). This increased perinuclear colocalization was inhibited by the presence of GST-RAP, indicating that it is dependent on $\alpha_2$M*/LRP1 binding and endocytosis (Supplemental Fig. S1). On the other hand, GFP-MT1-MMP and LRP1 colocalization was not visualized in regions near the cellular protrusions of $\alpha_2$M*-stimulated cells. Next, we detected that GFP-MT1-MMP was significantly colocalized with EEA1-positive vesicles (~55%), compatible with early endosomes, in MIO-M1 cells cultured in the presence of $\alpha_2$M* for 30 min with respect to nonstimulated cells (~15%; **Fig. 5**). Similarly, LRP1 also showed a significant increase of colocalization with EEA1 vesicles (~55%) in $\alpha_2$M*-stimulated cells compared with nonstimulated MIO-M1 cells (~35%). The merged image for GFP-MT1-MMP/LRP1/EEA1 staining indicates that the 3 proteins were highly colocalized in MIO-M1 cells stimulated with $\alpha_2$M*. Taken together, these results demonstrate that $\alpha_2$M* promoted MT1-MMP protein accumulation in early endosomes in association with LRP1.

To evaluate whether $\alpha_2$M* induced the endocytic recycling of MT1-MMP in MIO-M1 cells, we first examined the localization of this membrane protease in recycling compartments, using MIO-M1 cells cotransfected with RFP-wt-Rab11 and GFP-MT1-MMP. **Figure 6** shows that GFP-MT1-MMP significantly colocalized with RFP-wt-Rab11 (~40%) in MIO-M1 cells stimulated with $\alpha_2$M* for 30 min, with respect to nonstimulated cells (~20%). However, although LRP1 also showed a certain level of colocalization with Rab11-positive vesicles (~20%), this percentage was not significantly modified by $\alpha_2$M*. Similar results were also obtained when the recycling compartments were examined by continuous uptake of Alexa Fluor 594-conjugated transferrin (Tf) as a tracer of the endocytic recycling pathway for transferrin receptor (TfR) (ref. 46 and data not shown). Interestingly, an increased colocalization between GFP-MT1-MMP and RFP-wt-Rab11, but not between LRP1 and RFP-wt-Rab11, was also observed in cellular processes of MIO-M1 cells stimulated with $\alpha_2$M* when compared to nonstimulated cells (Supplemental Fig. S2). Finally, we evaluated the endocytic degradation pathway using a specific monoclonal antibody against Rab7 (late endosomes) and LysoTracker Red probes (acidic lysosome-like organelles). In both compartments, a low colocalization level (~10%) between GFP-MT1-MMP and LRP1 was found, which was not modified under $\alpha_2$M* stimulation (Supplemental Fig. S3). Thus, these results clearly indicate that $\alpha_2$M* induced MT1-MMP accumu-

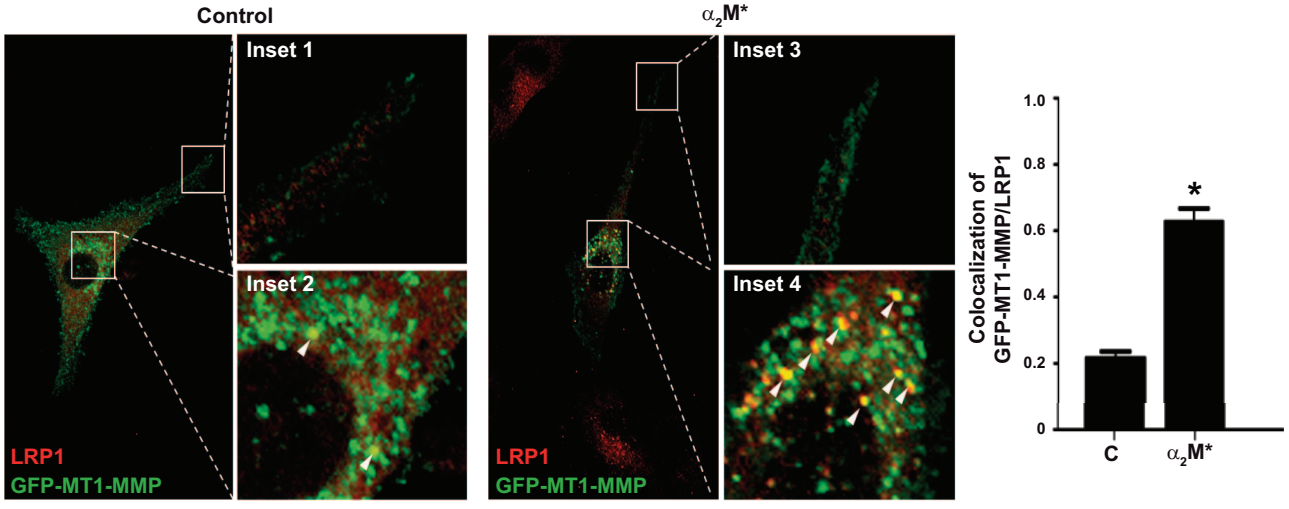


**Figure 4.** MT1-MMP and LRP1 colocalization is increased in MIO-M1 cells stimulated with $\alpha_2$M*. Each panel shows representative images obtained by confocal microscopy. MIO-M1 cells transfected with GFP-MT1-MMP were cultured in glass coverslips coated with collagen type I in the absence (control) or presence of $\alpha_2$M* (60 nM) for 1 h. Then, LRP1 was immunodetected using a mouse monoclonal LRP1 β-subunit antibody (clone 5A6). The overlaid images are magnifications of the protrusion (insets 1 and 3) and perinuclear regions (insets 2 and 4) of the cells (boxes) for GFP-MT1-MMP and LRP1 detection. In insets 2 and 4, GFP-MT1-MMP and LRP1 colocalizations are indicated by arrowheads. In contrast, colocalization between both proteins is not observed in border regions (insets 1 and 3). Quantification of colocalization levels between GFP-MT1-MMP and LRP1 was performed in the perinuclear region (insets 2 and 4) and is represented in the bar graph. Conditions of confocal microscopy and quantifications are detailed in Materials and Methods. Three independent experiments were performed in triplicate. *$P < 0.05$ *vs.* control (C).

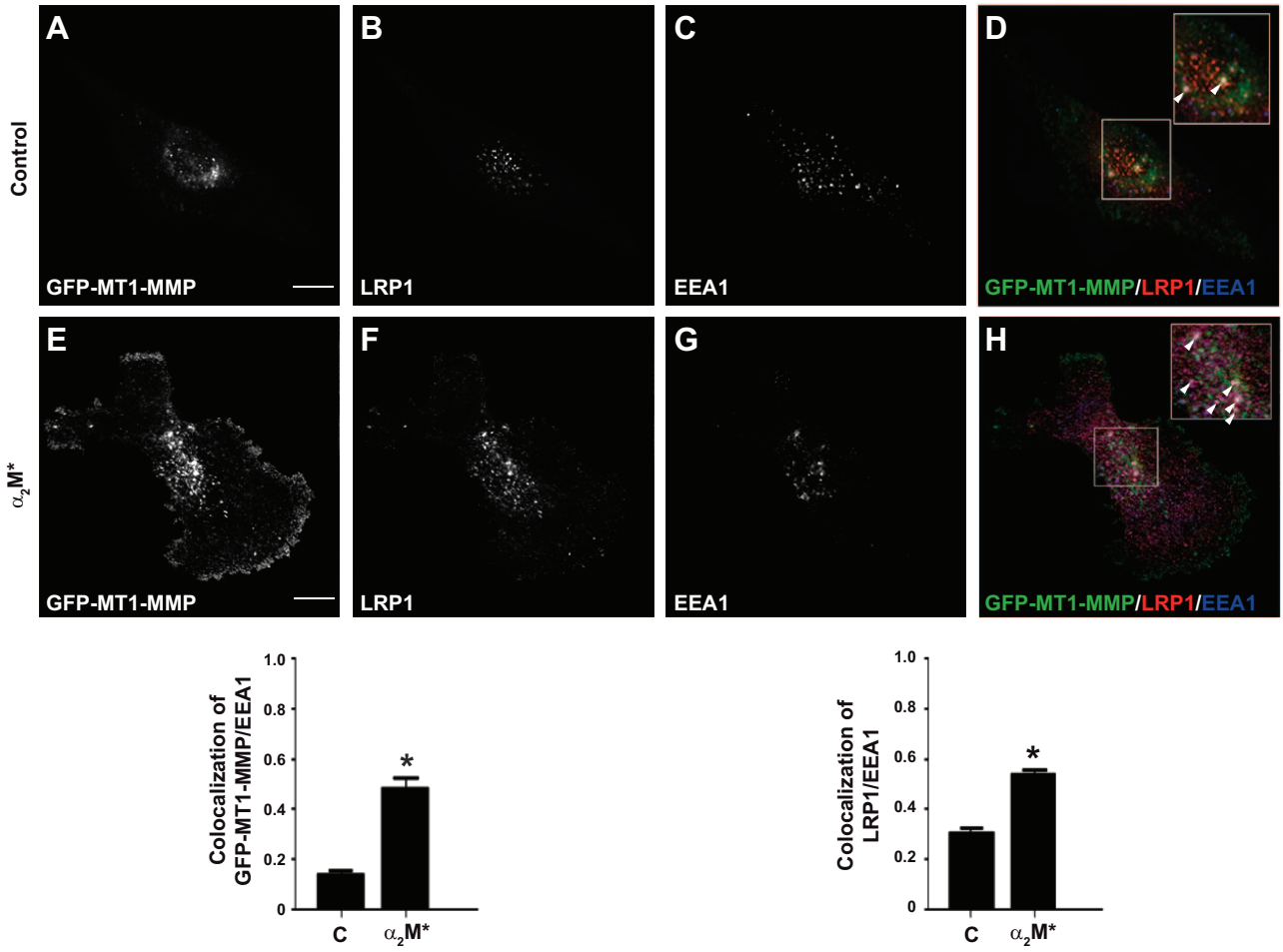


**Figure 5.** MT1-MMP and LRP1 are colocalizated in early endosomes (EEA1-positive vesicles) in MIO-M1 cells stimulated with $\alpha_2$M*. MIO-M1 cells transfected with GFP-MT1-MMP were cultured in glass coverslips coated with collagen type I in the absence (control; *A–D*) or presence of $\alpha_2$M* (60 nM; *E–H*) for 1 h. *A*, *E*) GFP-MT1-MMP. *B*, *F*) LRP1 immunodetection. *C*, *G*) EEA1 immunodetection. Quantification of the colocalization levels between GFP-MT1-MMP *vs.* EEA1 and LRP1 *vs.* EEA1 is represented in the bar graphs following the conditions detailed in Materials and Methods. *D*, *H*) Representative merged images of triple staining under control (*D*) and $\alpha_2$M* conditions (*H*). Insets: magnified images of the perinuclear region of the cells (boxed areas), where a triple colocalization between GFP-MT1-MMP, LRP1, and EEA1 is visualized (arrowheads). In panel *H*, it is observed that $\alpha_2$M* induced an increase in the colocalization of 3 proteins with respect to control (*D*). Scale bars = 10 μm. All results are representative of 3 independent experiments performed in triplicate. *$P < 0.05$ *vs.* control (C).

lation in Rab11-positive endocytic recycling compartments.

### $\alpha_2$M* increases the intracellular association between LRP1 and MT1-MMP

Considering that $\alpha_2$M* increased the colocalization of LRP1 and MT1-MMP, mostly in early endosomes, we investigated a possible molecular association between both membrane proteins using immunoprecipitation assays. **Figure 7*A*** shows the immunoblot for LRP1 when MT1-MMP was immunoprecipitated from protein extracts of MIO-M1 cells. Under these experimental conditions, LRP1 was immunodetected in nonstimulated cells, indicating that LRP1 and MT1-MMP proteins were associated at basal conditions in this type of cells. Interestingly, the amount of LRP1 coimmunoprecipitated with MT1-MMP increased in MIO-M1 cells cultured in the presence of $\alpha_2$M* for 1 h. Similarly, and as shown in Fig. 7*B*, the MT1-MMP immunoblot was significantly increased when LRP1 was immunoprecipitated in $\alpha_2$M*-stimulated MIO-M1 cells, with respect to nonstimulated cells. In this last case, a basal association between LRP1 and MT1-MMP proteins was also observed in cells cultured without $\alpha_2$M*. These data suggest that $\alpha_2$M* enhances the molecular association between MT1-MMP and LRP1, possibly in early endosomes.

### $\alpha_2$M* induces MT1-MMP intracellular traffic toward the plasma membrane by a Rab11-dependent pathway

To determine whether $\alpha_2$M* induced the intracellular traffic of MT1-MMP to the plasma membrane, a biotin-

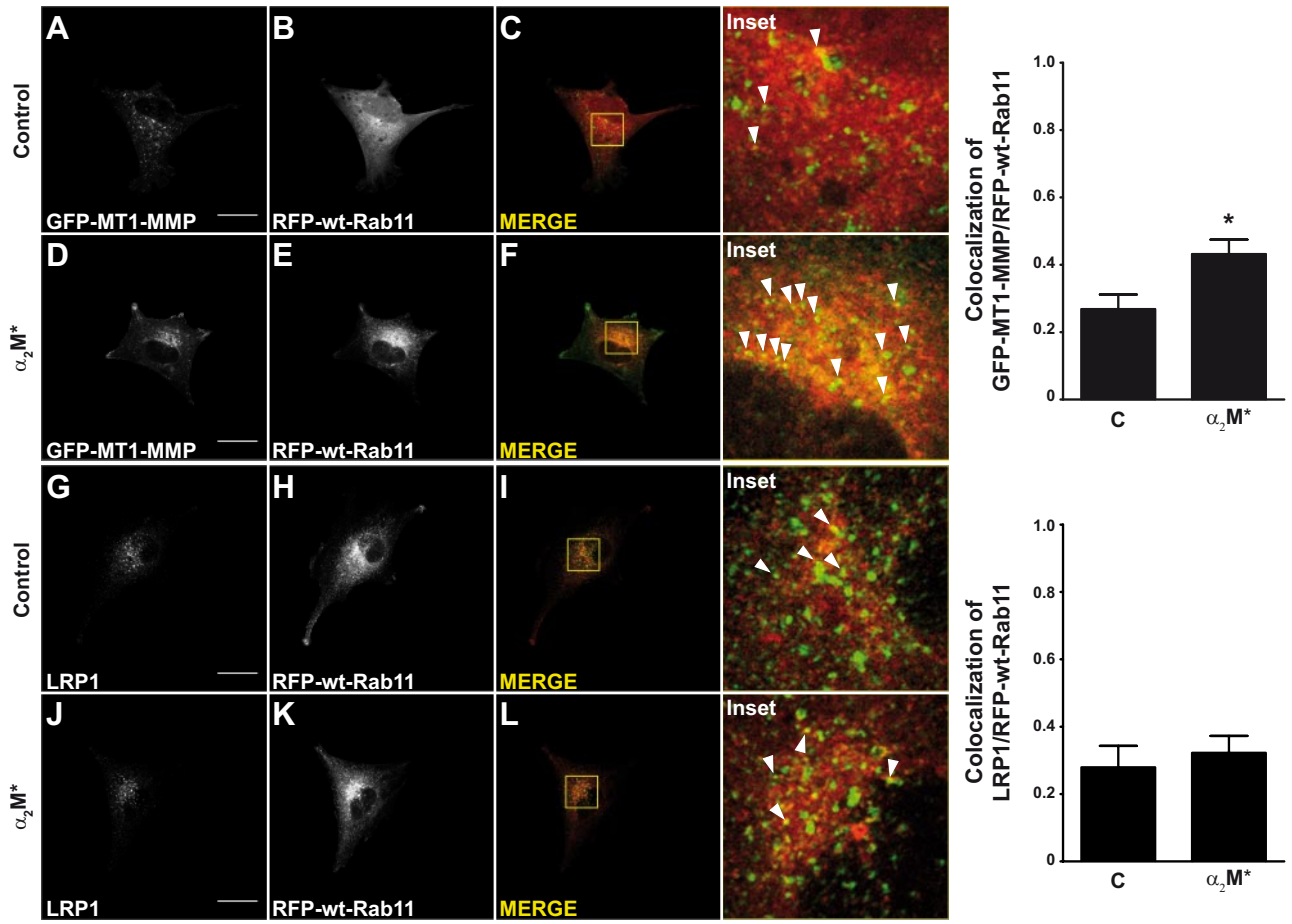


**Figure 6.** GFP-MT1-MMP and LRP1 localization in Rab11-positive recycling compartments in MIO-M1 cells stimulated with $\alpha_2$M*. MIO-M1 cells transfected with GFP-MT1-MMP and RFP-wt-Rab11 were cultured in glass coverslips coated with collagen type I in the absence (control; *A–C, G–I*) or presence of $\alpha_2$M* (60 nM; *D–F, J–L*) for 1 h. Then, LRP1 was immunodetected as indicated above. *A, D*) GFP-MT1-MMP. *G, J*) LRP1 immunodetection under control (*G*) and $\alpha_2$M* conditions (*J*). RFP-wt-Rab11-transfected cells in control (*B, H*) and $\alpha_2$M* conditions (*E, K*). Merged images for GFP-MT1-MMP/RFP-wt-Rab11 and LRP1/RFP-wt-Rab11 in control (*C, I*) and $\alpha_2$M* conditions (*F, L*). Insets: overlaid images are magnifications of the perinuclear region of cells (boxed areas), where the colocalization between GFP-MT1-MMP/RFP-wt-Rab11 and LRP1/RFP-wt-Rab11 is visualized (arrowheads). Quantitative colocalizations are represented by bar graphs following the conditions detailed in Materials and Methods. Three independent experiments were performed in triplicate. Scale bars = 10 μm. *$P < 0.05$ *vs.* control.

labeling cell surface protein assay was used. To carry this out, MIO-M1 cells were treated with $\alpha_2$M* for 1 h, followed by biotin labeling, as detailed in Materials and Methods. Using the protein extracts, an immunoprecipitation procedure for MT1-MMP was performed. **Figure 8*A*** shows that the biotin-labeled MT1-MMP was increased when the MIO-M1 cells were stimulated with $\alpha_2$M*. The biotin band for MT1-MMP was deduced by the molecular weight (~55 kDa) and by immunoblots using a specific antibody against MT1-MMP. Thus, these data indicate that $\alpha_2$M* induced MT1-MMP intracellular traffic toward the plasma membrane. In the same experiments, we were unable to detect biotin bands with molecular weights similar to LRP1-β- and LRP1-α-subunits, thereby demonstrating that MT1-MMP and LRP1 were not associated in the plasma membrane, which is in agreement with the results shown in Fig. 4.

To evaluate whether Rab11 was involved in the intracellular traffic of MT1-MMP to the plasma membrane induced by $\alpha_2$M*, MIO-M1 cells were transfected with a GFP plasmid (GFP), GFP-wild type Rab11 plasmid (GFP-wt-Rab11) or a dominant-negative mutant of Rab11 plasmid (GFP-Rab11S25N). When quantified by flow cytometry, ~65% of MIO-M1 cells were transfected with each plasmid (data not shown). Next, after $\alpha_2$M* stimulation, the biotin-labeling cell surface protein assay was performed. In this way, $\alpha_2$M* increased biotin-labeled MT1-MMP in cells transfected with GFP-wt-Rab11 (Fig. 8*A*) and GFP (Supplemental Fig. S2). However, when MIO-M1 cells were transfected with GFP-Rab11S25N, the increase in the biotin-labeled MT1-MMP band induced by $\alpha_2$M* was then abrogated. In addition, by confocal microscopy we observed that MT1-MMP cellular distribution to cellular protrusions was inhibited in GFP-Rab11S25N transfected MIO-M1 cells stimulated with $\alpha_2$M* (Fig. 8*B*). Interestingly, the presence of dominant-negative Rab11 in $\alpha_2$M*-stimulated cells promoted an increased accumulation of MT1-MMP in recycling compartments with respect to

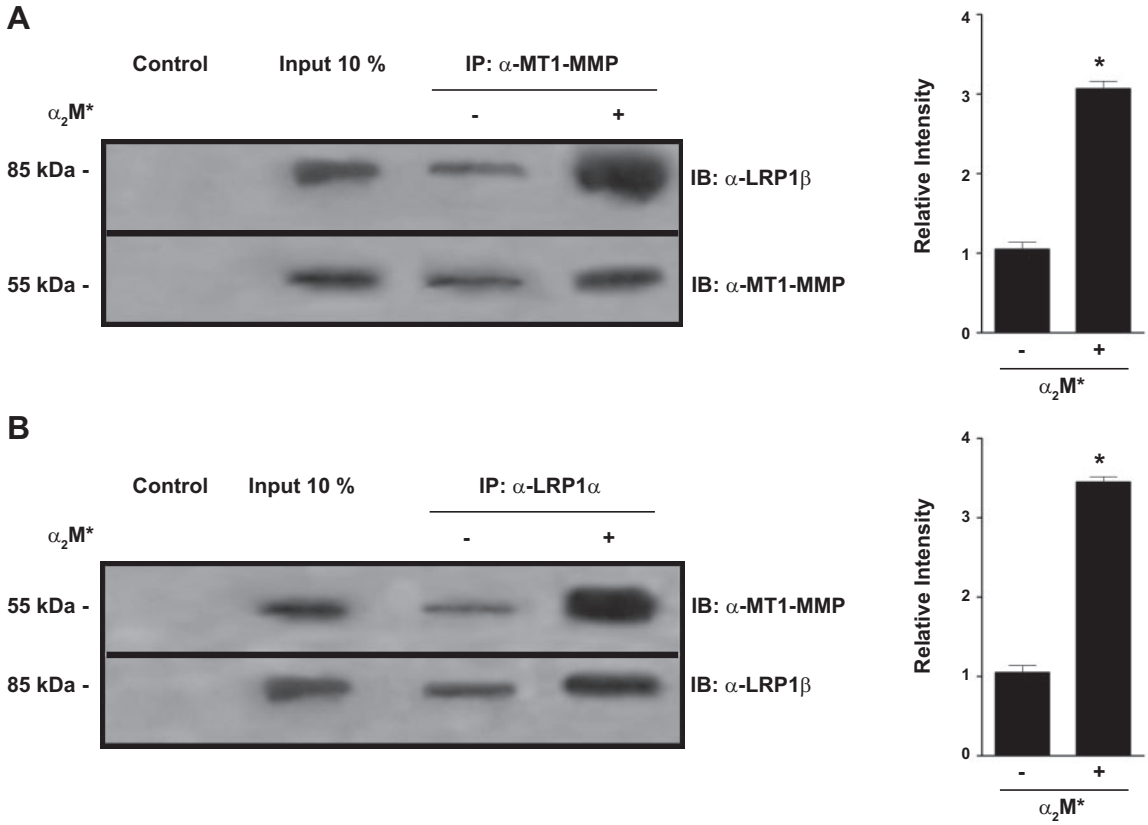


**Figure 7.** $\alpha_2$M* induces an increase in the molecular association between MT1-MMP and LRP1 in MIO-M1 cells. Cells were treated with $\alpha_2$M* (60 nM) for 1 h, and cell lysates were incubated at 4°C with either mouse monoclonal antibody anti-MT1-MMP (α-MT1-MMP) or mouse monoclonal antibody anti-LRP1 α-subunit (α-LRP1α) cross-linked to protein G-Sepharose magnetic beads, as detailed in Materials and Methods. Equal amounts of eluted proteins were resolved on SDS-PAGE and immunoblotted with either a mouse monoclonal antibody anti-LRP1 β-subunit (α-LRP1β) or mouse monoclonal antibody anti-MTI-MMP (α-MT1-MMP). A secondary HRP-conjugated antibody was utilized and revealed using a chemioluminiscense kit. Bands corresponding to $\alpha_2$M* nonstimulated (−) and stimulated (+) conditions were quantified by densitometric analysis and are represented in the bar graphs. In control conditions, cell lysates were incubated as above with a mouse nonimmune IgG cross-linked to protein G-Sepharose magnetic beads. *A*) Immunoprecipitation assay (IP) for MT1-MMP and immunoblotting (IB) for LRP1 and MT1-MMP. *B*) IP for LRP1 and IB for MT1-MMP and LRP1. All results are representative of 3 independent experiments performed in triplicate. $*P < 0.05$ *vs.* nonstimulated $\alpha_2$M* (−) condition.

nonstimulated cells. Thus, these results demonstrate that $\alpha_2$M*-induced MT1-MMP intracellular traffic to the plasma membrane by a Rab11-dependent pathway.

Finally, cellular migration and proMMP-2 activation induced by $\alpha_2$M* in Rab11 transiently transfected MIO-M1 cells (GFP-wt-Rab11 and GFP-Rab11S25N) were evaluated. **Figure 9*A*** shows a two-dimensional wound-scratch assay, where MIO-M1 cells transfected with GFP-wt-Rab11 presented increased cellular migration under $\alpha_2$M* stimulation when compared to nonstimulated cells. On the other hand, $\alpha_2$M* did not induce MIO-M1 cell migration in cells transfected with GFP-Rab11S25N. In addition, cell culture supernatants of Rab11-transfected MIO-M1 cells were analyzed by gelatin zymography. Figure 9*B* shows that $\alpha_2$M*-induced proMMP2 activation was abrogated in GFP-Rab11S25N transfected cells, whereas the active form of MMP-2 was observed in GFP-wt-Rab11 transfected cells stimulated with $\alpha_2$M*. Thus, taken together, these results demonstrate that $\alpha_2$M* *via* LRP1-induced MT1-MMP activation at the cell surface level through a Rab11-dependent pathway, which promoted MIO-M1 cell migration and proMMP2 activation.

## DISCUSSION

In the retina, MGCs play key structural and functional roles, and under physiological conditions these cells have a limited capability to migrate and proliferate. Nevertheless, in determined pathological abnormalities, MGCs can undergo functional and phenotypic changes, thereby acquiring the ability to migrate toward injured sites to promote retinal remodeling and cellular repopulation (41, 47). Although the regulatory mechanisms that promote this MGC migration are unclear, it has been proposed that ECM remodeling, produced by MMP-2 and MMP-9, may facilitate and induce the cellular migration of MGCs (22, 48). Furthermore, it has been suggested that MGCs are capable of re-entering the cell cycle, dedifferentiating and adopting characteristics of progenitor and stem cells.

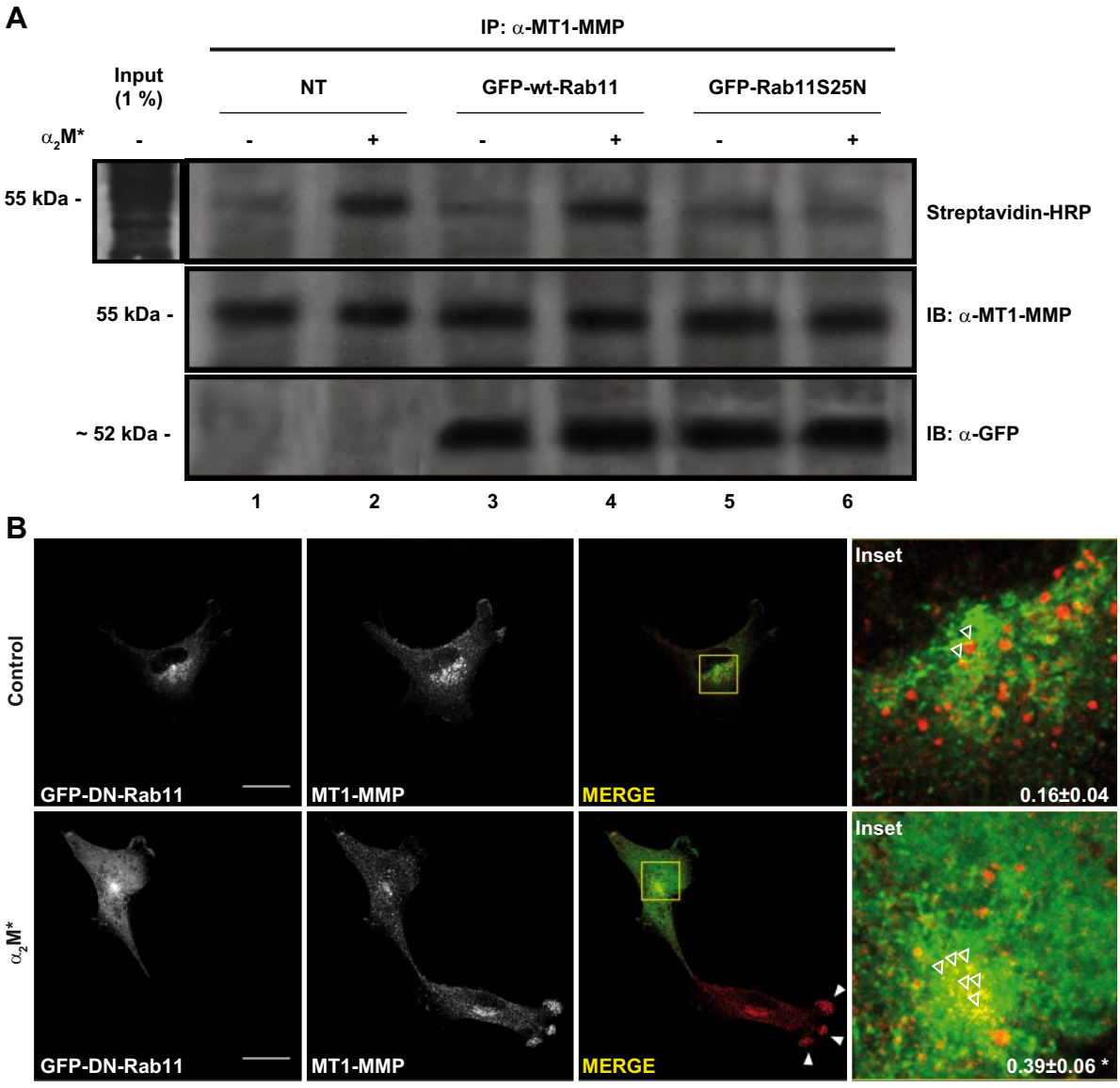


**Figure 8.** *A*) $\alpha_2$M* increases MT1-MMP expression at the cell surface level in MIO-M1 cells. Cells were treated with $\alpha_2$M* (60 nM) for 1 h, and the cell surface level of MT1-MMP was evaluated by a biotin-labeling protein assay. Then, the biotin MT1-MMP was immunoprecipitated (IP) with mouse anti-MT1-MMP antibody (α-MT1-MMP) from whole-cell lysates of nontransfected and Rab11-transfected MIO-M1 cells. Equal amounts of eluted proteins were resolved on SDS-PAGE, blotted with HRP-conjugated streptavidin and revealed by chemioluminiscense. IP for MT1-MMP in MIO-M1 cells that were not transfected (NT) or transfected with GFP-wt-Rab11 or GFP-Rab11S25N plasmids. Immunoblotting (IB) for MT1-MMP (α-MT1-MMP) and GFP (α-GFP) was carried out as IP and transfection controls, respectively. Input (1%) of biotinilated proteins is shown. *B*) MIO-M1 cells transfected with GFP-Rab11S25N (GFP-DN-Rab11) and stimulated with $\alpha_2$M* inhibit the MT1-MMP intracellular traffic to cellular processes and increases the MT1-MMP accumulation in Rab11-positive recycling compartments. MIO-M1 cells transfected with GFP-DN-Rab11 were cultured in glass coverslips coated with collagen type-I in the absence (control) or presence of $\alpha_2$M* (60 nM) for 1 h. Bottom panels show one nontransfected; it can be seen that the $\alpha_2$M*-induced MT1-MMP localization occurs toward cellular protrusions (solid arrowheads), whereas in the GFP-DN-Rab11-transfected cell, the MT1-MMP is accumulated in recycling compartments (boxed area) but not in cellular protrusions. Insets: overlaid images (inset) are magnifications of the perinuclear region of cells (boxed areas) for GFP-DN-Rab11 and MT1-MMP, where the colocalization between GFP-DN-Rab11 and MT1-MMP is visualized (open arrowheads). Mean ± SEM of colocalization levels between GFP-DN-Rab11 and MT1-MMP performed in the perinuclear region (boxes) are indicated. These results and images are representative of 3 independent experiments. Scale bars = 10 μm. *$P < 0.05$ *vs.* control.

These later cells can migrate to the damaged retinal tissue and produce new neurons following specific types of retinal injury, a process collectively known as transdifferentiation (49, 50). In addition, $\alpha_2$M has been detected at high levels in various retinal degenerative disorders, such as glaucoma (51, 52) and ischemic proliferative diseases (11, 13). In these retinas, native $\alpha_2$M may interact with released active proteases and form complexes ($\alpha_2$M*), which then binds to LRP1 (1). It is known that $\alpha_2$M*-LRP1 interaction, despite inducing

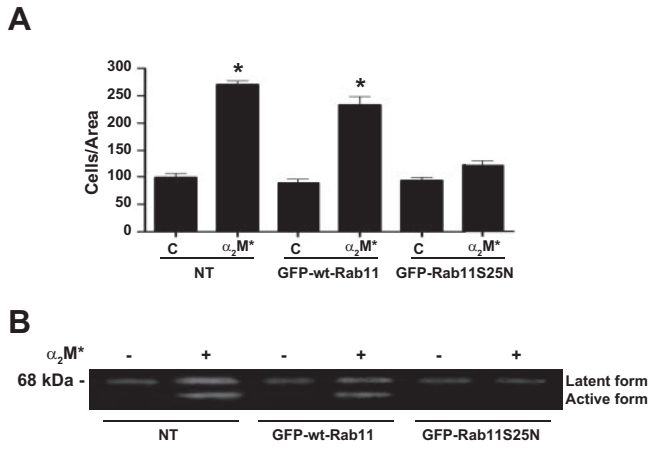


**Figure 9.** *A*) Cellular migration induced by $\alpha_2$M* is inhibited in MIO-M1 cells transfected with a dominant-negative version of Rab11 (GFP-Rab11S25N). Nontransfected (NT) and transfected (GFP-wt-Rab11 and GFP-Rab11S25N) cells were cultured for 12 h in serum-free DMEM, in the absence or presence of $\alpha_2$M* (60 nM). Wound-scratch assays were performed in cells cultured on plates coated with collagen type I, as was described in Materials and Methods. Bar graph represents mean values of the cell number invading the area of the wound (cells/area). Three independent experiments were performed in triplicate. *$P < 0.05$ *vs.* control (C). *B*) The proMMP-2 activation induced by $\alpha_2$M* is inhibited in MIO-M1 cells transfected with a dominant-negative version of Rab11 (GFP-Rab11S25N). Nontransfected and transfected (GFP-wt-Rab11 and GFP-Rab11S25N) cells were cultured in serum-free DMEM, in the absence (−) or presence (+) of $\alpha_2$M* (60 nM) for 1 h. Cell culture supernatants were collected and analyzed by gelatin zymography assay, as detailed in Material and Methods. MIO-M1 cells, transfected with GFP-Rab11S25N, show that the $\alpha_2$M*-induced proMMP-2 activation (latent form) to either intermediate or active MMP-2 (active form) is inhibited with respect to nontransfected and GFP-wt-Rab11 transfected conditions. The proMMP-2 molecular weight (68 kDa) is indicated. Three independent experiments were performed.

endocytosis of the inhibitor-protease complex, also activates different intracellular signaling pathways (5, 6). In this regard, we have recently demonstrated that $\alpha_2$M* promoted GFAP expression in MIO-M1 cells, which was associated with the cellular activation of these retinal cells (7). In the present study, we found that $\alpha_2$M* induced cellular migration and proMMP-2 activation through LRP1 in MIO-M1 cells.

In addition to its function as a protease inhibitor, $\alpha_2$M may reversibly bind growth factors, such as the nerve growth factor (NGF). These interactions involve the internal part of $\alpha_2$M molecule, but not the C-terminal receptor binding domain (RBD) that recognizes LRP1 (53, 54). The binding of NGF to $\alpha_2$M blocked the signaling activation of Akt and ERK/MAP kinase (53) and neutralized the neuroprotective action induced by this neurothrophin (52). For this reason, it has been suggested that in glaucoma $\alpha_2$M may have a neurotoxic function through its ability to block the neurotrophic action of NGF (53). Interestingly, our results indicate that $\alpha_2$M*, through its RBD, may be an inductor factor of MGC migration, thus facilitating cellular repopulation into the damaged host retina. However, additional studies are required in order to explain the migratory properties of $\alpha_2$M* in glial cells with different retinal pathologies.

It has been previously reported that $\alpha_2$M*-LRP1 interaction induces cellular proliferation in macrophages (5), releases proinflammatory factors in Schwann cells (55), and inhibits NGF-induced neurite outgrowth in PC12 cells (33). In the present work, we observed that MIO-M1 cells acquired migratory properties under $\alpha_2$M* stimulation, which was characterized by the cellular redistribution of MT1-MMP to cellular protrusions. In this way, it was established that the migration of normal and malignant cells depended on MT1-MMP accumulation at the membrane protrusions (also termed podosomes and invadopodias), which is required for the focal pericellular degradation of ECM (56). The activity of MT1-MMP in these membrane protrusions is, in part, dependent on the endocytic recycling of this active protease, which may be mediated by a Rab11-dependent pathway (57–59). Herein, we showed that $\alpha_2$M* induced intracellular accumulation of MT1-MMP in early and recycling endosomes, as well as intracellular trafficking to the plasma membrane mediated by Rab11. Using a dominant-negative version of Rab11 (GFP-Rab11S25N), we also demonstrated that $\alpha_2$M*-induced cell migration of MIO-M1 cells and proMMP-2 activation were completely abrogated, indicating that this small GTPase plays a key role in maintaining active MT1-MMP at the cell surface. In addition, by a biotin labeling cell surface protein assay, it was found that GFP-Rab11S25N also inhibited the MT1-MMP traffic to the plasma membrane induced by $\alpha_2$M* stimulation. Under these experimental conditions MT1-MMP was mainly accumulated in recycling compartments, indicating that the intracellular traffic of this protease to the plasma membrane induced by $\alpha_2$M* is routed from a Rab11-dependent pathway. In another report, it was shown that MT1-MMP may be trafficked toward membrane protrusions through an exocytic route dependent on Rab8 (but not Rab11), where it mediated the cellular migration of MDA-MB-23 adenocarcinoma cells in two- and three-dimensional collagen type I matrices (30). These researchers observed that the exocytic route of MT1-MMP to the plasma membrane was from VSV-G/Rab8-positive vesicles, but not Rab11-positive compartments in cells cultured in collagen type-I matrices. Nevertheless, Rab11-dependent recycling pathway of MT1-MMP seemed to be activated when the same cells were cultured in coverslips without collagen type-I (30). Thus, it has been suggested that the intracellular traffic of MT1-MMP activity toward the cell surface, and its participation in cellular migration, may be dependent on the tumoral or nontumoral characteristics of cells, as well as on the presence of determined extracellular factors that induce cellular migration, such as collagen type I. Interestingly, in our work, the cellular migration of MIO-M1 cells in two-dimensional collagen type I matrices was significantly induced by $\alpha_2$M* respect to

cells cultured without stimulus. In addition, unpublished results from our laboratory showed that $\alpha_2$M* also promoted the cellular migration of MIO-M1 cells when cultured in coverslip without collagen type-1 or adsorbed with other ECM components, such as laminin. Taken together, our results indicate that collagen type-I *per se* is not an inductor factor for the cellular migration of MIO-M1 cells, which could explain in part the MT1-MMP traffic by a Rab11-dependent (but not Rab8-dependent) pathway. Thus, we conclude that $\alpha_2$M* regulated the intracellular traffic of MT1-MMP toward the cellular protrusions and induced cellular migration and proMMP-2 activation in MGCs through a recycling route dependent on Rab11. In the future, it would be interesting to investigate whether $\alpha_2$M* may also activate a Rab11-dependent pathway for MT1-MMP trafficking and its effect on cellular migration in malignant cells.

LRP1 is an endocytic and cell-signaling receptor for diverse ligands, and it can regulate cellular functions of other membrane proteins, such as uPAR (9) and PDGFRβ (10). However, pathways by which LRP1 can control cell surface activity of MT1-MMP remain less clear. In our study, we observed that LRP1 was mostly associated with MT1-MMP in intracellular compartments, which was significantly increased in cells stimulated with $\alpha_2$M*. By confocal microscopy, we found that LRP1 and MT1-MMP were mainly colocalized in early endosomes, which seems to indicate that $\alpha_2$M* induced, in addition to LRP1, the endocytosis of MT1-MMP. As it is well established that MT1-MMP is internalized by clathrin- and non-clathrin-dependent endocytosis (45), whereas the $\alpha_2$M*-LRP1 complex is only internalized by a clathrin-dependent endocytosis (3), we hypothesize that both membrane proteins are internalized by different endocytic routes and accumulated in early endosomes. However, the mechanism that regulates the MT1-MMP internalization induced by $\alpha_2$M* is unknown. It has been shown that MT1-MMP endocytosis occurs when the Thr-567 residue is phos-

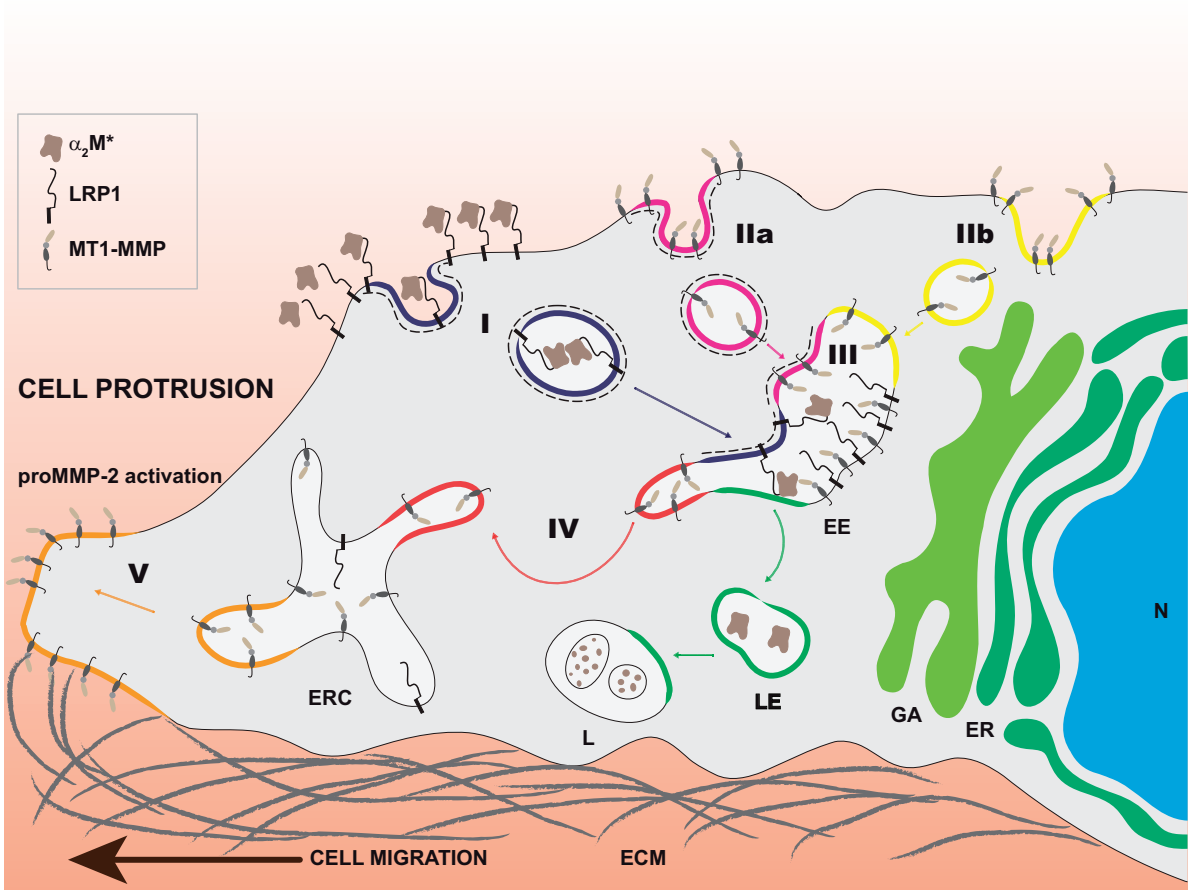


**Figure 10.** Schematic model of the MT1-MMP regulation induced by $\alpha_2$M*/LRP1 interaction. *I*) $\alpha_2$M* binds LRP1, and the ligand-receptor complex is internalized by a clathrin-dependent endocytosis (blue). *II*) MT1-MMP is internalized through two putative pathways: clathrin-dependent (*IIa*, pink) and non-clathrin-dependent endocytosis (IIb, yellow). *III*) $\alpha_2$M*-LRP1 complex and MT1-MMP are accumulated in early endosomes (EE), where the ligand ($\alpha_2$M*) is released of LRP1 to degradation pathways (green): late endosomes (LE) and lysosomes (L). *IV*) MT1-MMP-enriched EEs (red) are differentially trafficked and fused with endocytic recycling compartments (ERC) where MT1-MMP is accumulated. *V*) On the other hand, LRP1 is apparently accumulated in EE, and MT1-MMP is trafficked (orange) to the plasma membrane through a Rab11-dependent pathway. Finally, this MT1-MMP regulation promotes the MGC migration and proMMP-2 activation. In this model, the possibility of an MT1-MMP traffic loop between the Golgi apparatus (GA) and ERC is not excluded. ER, endoplasmic reticulum; N, nucleus.

phorylated by protein kinase Cα (PKCα; ref. 60). Interestingly, PKCα also induces serine and threonine phosphorylations in the intracytoplasmatic domain of LRP1, thereby promoting interaction with adaptor proteins such as Dab-1 and CED-6/GULP, which modulate the endocytic and signaling function of this receptor (61). Recently, we found that the $\alpha_2$M*-LRP1 interaction induced different intracellular signaling pathways, including PKCα (6), which, in fact, might be involved in the Thr-567 phosphorylation of MT1-MMP, thus promoting its endocytosis and accumulation in early endosomes. Furthermore, both LRP1 and MT1-MMP were immunoprecipitated in nonstimulated cells, indicating that both proteins are intermolecularly associated, with this association being increased under $\alpha_2$M* stimulus. However, we did not determine whether this LRP1/MT1-MMP interaction was direct or was mediated by intermediate molecules or adaptor proteins. In this regard, a recent report has demonstrated that the MT1-MMP catalytic domain can directly interact with the LRP1 α subunit, thereby promoting its proteolytic shedding at the cell surface level (62). In our case, we were unable to detect colocalization between the LRP1 β subunit and MT1-MMP at the plasma membrane, suggesting that this type of interaction does not occur in MIO-M1 cells cultured both in either the absence or presence of $\alpha_2$M*. Moreover, intracytoplasmatic domains of the LRP1 β subunit and MT1-MMP can interact with several adaptor proteins (61, 63). Therefore, one possibility is that the LRP1/MT1-MMP association may be mediated by a common adaptor protein, similar to FE65, which is known to mediate the interaction between LRP1 and the amyloid precursor protein (APP; ref. 64). However, additional studies are needed to investigate this hypothesis.

Finally, in the present work, we also found that active MT1-MMP, but not LRP1, was increased in recycling Rab11-positive compartments under $\alpha_2$M* stimulation in MIO-M1 cells. These cellular distributions of both proteins suggest that $\alpha_2$M* induced the recycling of MT1-MMP back to the cell surface by a recycling pathway, whereas LRP1 was apparently kept in early endosomes. Interestingly, as mentioned above, MT1-MMP and LRP1 mainly colocalized in early endosomes, where the differential intracellular trafficking of MT1-MMP and LRP1 could be regulated. This possibility may be supported by previous studies that reported that LRP1 may interact and regulate the function of PDGF receptor (PDGF-Rβ) in early endosomes, modulating its intracellular signaling activity (65). In the same way, LRP1 and MT1-MMP are accumulated in early endosomes by $\alpha_2$M* induction, and then MT1-MMP, but not LRP1, is specifically trafficked to recycled compartments and plasma membrane through a Rab11-dependent pathway. However, further experiments are needed to establish whether LRP1 is also recycled to the plasma membrane under $\alpha_2$M* stimulation. In addition, the accumulation of MT1-MMP in recycling compartments may also involve a newly synthesized MT1-MMP that travels through the biosynthetic pathway and accumulates with preexisting MT1-MMP molecules internalized from the cell surface (45). However, in our study, we were unable to inhibit $\alpha_2$M*-induced MT1-MMP traffic to the plasma membrane in MIO-M1 cells previously treated with cycloheximide, an inhibitor of protein synthesis (data not shown). Moreover, as $\alpha_2$M*-induced MT1-MMP redistribution to cellular protrusions and its trafficking to the plasma membrane occurred at relatively short times (between 30 and 60 min) after $\alpha_2$M* stimulus, it is unlikely that an MT1-MMP contribution from the biosynthetic pathway could occur. Further studies should now be conducted in order to evaluate the $\alpha_2$M* effect on the newly synthesized MT1-MMP and its contribution to the traffic toward the plasma membrane in MIO-M1 cells.

The results of our current investigation are summarized in **Fig. 10**, revealing a novel pathway in the regulation of MT1-MMP induced by $\alpha_2$M*. In this model, only the endocytic recycling route of MT1-MMP that is induced by the $\alpha_2$M*-LRP1 interaction is highlighted. Related to this, we suggest that $\alpha_2$M* is an extracellular factor that promotes MGC migration and proMMP2 activation. We also proposed that $\alpha_2$M*-LRP1 is also an extremely sensitive system for rapid and localized MT1-MMP mobilization. Thus, our results may have clinical and therapeutic connotations in retinal disorders that are deleterious for the human vision, such as in PDR and PVR. FJ

This work was supported in part by Secretaría de Ciencia y Tecnología de la Universidad Nacional de Córdoba (SECyT-UNC) grants 214/10 and 26/1169/08, Fondo para la Investigación Científica y Tecnológica (FONCyT): Préstamo BID Proyecto de Investigación en Ciencia y Tecnología (PICT) grant 06–01207, proyecto de Investigación en Ciencia y Tecnología Orientados (PICTO)-Glaxo grant 2012-0084, and Consejo Nacional de Investigaciones Cientificas y Tecnicas (CONICET) Proyecto de Investigación Plurianual (PIP) grant 112–200801-02067. P.B. and J.J-F. are doctoral fellows of CONICET. M.C.S. and G.A.C. are members of the Research Career of CONICET. The authors thank Dr. Paul D. Hobson, native speaker, for revising the manuscript.

## REFERENCES

1. Chu, C. T., and Pizzo, S. V. (1994) alpha 2-Macroglobulin, complement, and biologic defense: antigens, growth factors, microbial proteases, and receptor ligation. *Lab. Invest.* **71,** 792–812
2. Hussain, M. M., Strickland, D. K., and Bakillah, A. (1999) The mammalian low-density lipoprotein receptor family. *Annu. Rev. Nutr.* **19,** 141–172
3. Herz, J., and Strickland, D. K. (2001) LRP: a multifunctional scavenger and signaling receptor. *J. Clin. Invest.* **108,** 779–784
4. Gorovoy, M., Gaultier, A., Campana, W. M., Firestein, G. S., and Gonias, S. L. (2010) Inflammatory mediators promote production of shed LRP1/CD91, which regulates cell signaling and cytokine expression by macrophages. *J. Leukoc. Biol.* **88,** 769–778
5. Bonacci, G. R., Caceres, L. C., Sanchez, M. C., and Chiabrando, G. A. (2007) Activated alpha(2)-macroglobulin induces cell proliferation and mitogen-activated protein kinase activation by LRP-1 in the J774 macrophage-derived cell line. *Arch. Biochem. Biophys.* **460,** 100–106
6. Caceres, L. C., Bonacci, G. R., Sanchez, M. C., and Chiabrando, G. A. (2010) Activated alpha(2) macroglobulin induces matrix metalloproteinase 9 expression by low-density lipoprotein re-

ceptor-related protein 1 through MAPK-ERK1/2 and NF-κB activation in macrophage-derived cell lines. *J. Cell. Biochem.* **111,** 607–617
7. Barcelona, P. F., Ortiz, S. G., Chiabrando, G. A., and Sanchez, M. C. (2011) α2-Macroglobulin induces glial fibrillary acidic protein expression mediated by low-density lipoprotein receptor-related protein 1 in Muller cells. *Invest. Ophthalmol. Vis. Sci.* **52,** 778–786
8. Laatsch, A., Panteli, M., Sornsakrin, M., Hoffzimmer, B., Grewal, T., and Heeren, J. (2012) Low-density lipoprotein receptor-related protein 1-dependent endosomal trapping and recycling of apolipoprotein E. *PLoS One* **7,** e29385
9. Gonias, S. L., Gaultier, A., and Jo, M. (2011) Regulation of the urokinase receptor (uPAR) by LDL receptor-related protein-1 (LRP1). *Curr. Pharm. Des.* **17,** 1962–1969
10. Boucher, P., Gotthardt, M., Li, W. P., Anderson, R. G., and Herz, J. (2003) LRP: role in vascular wall integrity and protection from atherosclerosis. *Science* **300,** 329–332
11. Sanchez, M. C., Barcelona, P. F., Luna, J. D., Ortiz, S. G., Juarez, P. C., Riera, C. M., and Chiabrando, G. A. (2006) Low-density lipoprotein receptor-related protein-1 (LRP-1) expression in a rat model of oxygen-induced retinal neovascularization. *Exp. Eye Res.* **83,** 1378–1385
12. Sanchez, M. C., Luna, J. D., Barcelona, P. F., Gramajo, A. L., Juarez, P. C., Riera, C. M., and Chiabrando, G. A. (2007) Effect of retinal laser photocoagulation on the activity of metalloproteinases and the $\alpha_2$-macroglobulin proteolytic state in the vitreous of eyes with proliferative diabetic retinopathy. *Exp. Eye Res.* **85,** 644–650
13. Barcelona, P. F., Luna, J. D., Chiabrando, G. A., Juarez, C. P., Bhutto, I. A., Baba, T., McLeod, D. S., Sanchez, M. C., and Lutty, G. A. (2010) Immunohistochemical localization of low density lipoprotein receptor-related protein 1 and $\alpha_2$-Macroglobulin in retinal and choroidal tissue of proliferative retinopathies. *Exp. Eye Res.* **91,** 264–272
14. Hollborn, M., Krausse, C., Iandiev, I., Yafai, Y., Tenckhoff, S., Bigl, M., Schnurrbusch, U. E., Limb, G. A., Reichenbach, A., Kohen, L., Wolf, S., Wiedemann, P., and Bringmann, A. (2004) Glial cell expression of hepatocyte growth factor in vitreoretinal proliferative disease. *Lab. Invest.* **84,** 963–972
15. Lewis, G. P., Matsumoto, B., and Fisher, S. K. (1995) Changes in the organization and expression of cytoskeletal proteins during retinal degeneration induced by retinal detachment. *Invest. Ophthalmol. Vis. Sci.* **36,** 2404–2416
16. Sethi, C. S., Lewis, G. P., Fisher, S. K., Leitner, W. P., Mann, D. L., Luthert, P. J., and Charteris, D. G. (2005) Glial remodeling and neural plasticity in human retinal detachment with proliferative vitreoretinopathy. *Invest. Ophthalmol. Vis. Sci.* **46,** 329–342
17. Wang, Y., Smith, S. B., Ogilvie, J. M., McCool, D. J., and Sarthy, V. (2002) Ciliary neurotrophic factor induces glial fibrillary acidic protein in retinal Muller cells through the JAK/STAT signal transduction pathway. *Curr. Eye Res.* **24,** 305–312
18. Kim, I. B., Kim, K. Y., Joo, C. K., Lee, M. Y., Oh, S. J., Chung, J. W., and Chun, M. H. (1998) Reaction of Muller cells after increased intraocular pressure in the rat retina. *Exp. Brain Res.* **121,** 419–424
19. Xue, L. P., Lu, J., Cao, Q., Hu, S., Ding, P., and Ling, E. A. (2006) Muller glial cells express nestin coupled with glial fibrillary acidic protein in experimentally induced glaucoma in the rat retina. *Neuroscience* **139,** 723–732
20. Newman, E., and Reichenbach, A. (1996) The Muller cell: a functional element of the retina. *Trends Neurosci.* **19,** 307–312
21. Guidry, C. (2005) The role of Muller cells in fibrocontractive retinal disorders. *Prog. Retinal Eye Res.* **24,** 75–86
22. Limb, G. A., Daniels, J. T., Pleass, R., Charteris, D. G., Luthert, P. J., and Khaw, P. T. (2002) Differential expression of matrix metalloproteinases 2 and 9 by glial Muller cells: response to soluble and extracellular matrix-bound tumor necrosis factor-alpha. *Am. J. Pathol.* **160,** 1847–1855
23. Lewis, G., Mervin, K., Valter, K., Maslim, J., Kappel, P. J., Stone, J., and Fisher, S. (1999) Limiting the proliferation and reactivity of retinal Muller cells during experimental retinal detachment: the value of oxygen supplementation. *Am. J. Ophthalmol.* **128,** 165–172
24. Kimura, H., Spee, C., Sakamoto, T., Hinton, D. R., Ogura, Y., Tabata, Y., Ikada, Y., and Ryan, S. J. (1999) Cellular response in subretinal neovascularization induced by bFGF-impregnated microspheres. *Invest. Ophthalmol. Vis. Sci.* **40,** 524–528
25. Noda, K., Ishida, S., Inoue, M., Obata, K., Oguchi, Y., Okada, Y., and Ikeda, E. (2003) Production and activation of matrix metalloproteinase-2 in proliferative diabetic retinopathy. *Invest. Ophthalmol. Vis. Sci.* **44,** 2163–2170
26. Strongin, A. Y. (2010) Proteolytic and non-proteolytic roles of membrane type-1 matrix metalloproteinase in malignancy. *Biochim. Biophys. Acta* **1803,** 133–141
27. Seiki, M., and Yana, I. (2003) Roles of pericellular proteolysis by membrane type-1 matrix metalloproteinase in cancer invasion and angiogenesis. *Cancer Sci.* **94,** 569–574
28. Yana, I., and Weiss, S. J. (2000) Regulation of membrane type-1 matrix metalloproteinase activation by proprotein convertases. *Mol. Biol. Cell* **11,** 2387–2401
29. Schram, K., Ganguly, R., No, E. K., Fang, X., Thong, F. S., and Sweeney, G. (2011) Regulation of MT1-MMP and MMP-2 by leptin in cardiac fibroblasts involves Rho/ROCK-dependent actin cytoskeletal reorganization and leads to enhanced cell migration. *Endocrinology* **152,** 2037–2047
30. Bravo-Cordero, J. J., Marrero-Diaz, R., Megias, D., Genis, L., Garcia-Grande, A., Garcia, M. A., Arroyo, A. G., and Montoya, M. C. (2007) MT1-MMP proinvasive activity is regulated by a novel Rab8-dependent exocytic pathway. *EMBO J.* **26,** 1499–1510
31. Limb, G. A., Salt, T. E., Munro, P. M., Moss, S. E., and Khaw, P. T. (2002) In vitro characterization of a spontaneously immortalized human Muller cell line (MIO-M1). *Invest. Ophthalmol. Vis. Sci.* **43,** 864–869
32. Chiabrando, G., Bonacci, G., Sanchez, C., Ramos, A., Zalazar, F., and Vides, M. A. (1997) A procedure for human pregnancy zone protein (and human alpha 2-macroglobulin) purification using hydrophobic interaction chromatography on phenyl-sepharose CL-4B column. *Protein Expr. Purif.* **9,** 399–406
33. Chiabrando, G. A., Sanchez, M. C., Skornicka, E. L., and Koo, P. H. (2002) Low-density lipoprotein receptor-related protein mediates in PC12 cell cultures the inhibition of nerve growth factor-promoted neurite outgrowth by pregnancy zone protein and alpha2-macroglobulin. *J. Neurosci. Res.* **70,** 57–64
34. Bu, G., Geuze, H. J., Strous, G. J., and Schwartz, A. L. (1995) 39 kDa receptor-associated protein is an ER resident protein and molecular chaperone for LDL receptor-related protein. *EMBO J.* **14,** 2269–2280
35. Sanchez, M. C., Chiabrando, G. A., and Vides, M. A. (2001) Pregnancy zone protein-tissue-type plasminogen activator complexes bind to low-density lipoprotein receptor-related protein (LRP). *Arch. Biochem. Biophys.* **389,** 218–222
36. Cao, J., Kozarekar, P., Pavlaki, M., Chiarelli, C., Bahou, W. F., and Zucker, S. (2004) Distinct roles for the catalytic and hemopexin domains of membrane type 1-matrix metalloproteinase in substrate degradation and cell migration. *J. Biol. Chem.* **279,** 14129–14139
37. Llorente-Cortes, V., Otero-Vinas, M., and Badimon, L. (2002) Differential role of heparan sulfate proteoglycans on aggregated LDL uptake in human vascular smooth muscle cells and mouse embryonic fibroblasts. *Arterioscler. Thromb. Vasc. Biol.* **22,** 1905–1911
38. Liang, C. C., Park, A. Y., and Guan, J. L. (2007) In vitro scratch assay: a convenient and inexpensive method for analysis of cell migration in vitro. *Nat. Prot.* **2,** 329–333
39. Kleiner, D. E., and Stetler-Stevenson, W. G. (1994) Quantitative zymography: detection of picogram quantities of gelatinases. *Anal. Biochem.* **218,** 325–329
40. Bolte, S., and Cordelieres, F. P. (2006) A guided tour into subcellular colocalization analysis in light microscopy. *J. Microsc.* **224,** 213–232
41. Romo, P., Madigan, M. C., Provis, J. M., and Cullen, K. M. (2011) Differential effects of TGF-β and FGF-2 on in vitro proliferation and migration of primate retinal endothelial and Muller cells. *Acta Ophthalmol.* **89,** e263–268
42. Seiki, M., Koshikawa, N., and Yana, I. (2003) Role of pericellular proteolysis by membrane-type 1 matrix metalloproteinase in cancer invasion and angiogenesis. *Cancer Metastasis Rev.* **22,** 129–143
43. Frittoli, E., Palamidessi, A., Disanza, A., and Scita, G. (2011) Secretory and endo/exocytic trafficking in invadopodia formation: the MT1-MMP paradigm. *Eur. J. Cell Biol.* **90,** 108–114

44. Tang, B. L., and Ng, E. L. (2009) Rabs and cancer cell motility. *Cell Motil. Cytoskel.* **66,** 365–370
45. Poincloux, R., Lizarraga, F., and Chavrier, P. (2009) Matrix invasion by tumour cells: a focus on MT1-MMP trafficking to invadopodia. *J. Cell Sci.* **122,** 3015–3024
46. Maxfield, F. R., and McGraw, T. E. (2004) Endocytic recycling. *Nat. Rev. Mol. Cell Biol.* **5,** 121–132
47. Bull, N. D., Limb, G. A., and Martin, K. R. (2008) Human Muller stem cell (MIO-M1) transplantation in a rat model of glaucoma: survival, differentiation, and integration. *Invest. Ophthalmol. Vis. Sci.* **49,** 3449–3456
48. Tackenberg, M. A., Tucker, B. A., Swift, J. S., Jiang, C., Redenti, S., Greenberg, K. P., Flannery, J. G., Reichenbach, A., and Young, M. J. (2009) Muller cell activation, proliferation and migration following laser injury. *Mol. Vis.* **15,** 1886–1896
49. Ooto, S., Akagi, T., Kageyama, R., Akita, J., Mandai, M., Honda, Y., and Takahashi, M. (2004) Potential for neural regeneration after neurotoxic injury in the adult mammalian retina. *Proc. Natl. Acad. Sci. U. S. A.* **101,** 13654–13659
50. Fischer, A. J., and Reh, T. A. (2001) Muller glia are a potential source of neural regeneration in the postnatal chicken retina. *Nat. Neurosci.* **4,** 247–252
51. Shi, Z., Rudzinski, M., Meerovitch, K., Lebrun-Julien, F., Birman, E., Di Polo, A., and Saragovi, H. U. (2008) Alpha2-macroglobulin is a mediator of retinal ganglion cell death in glaucoma. *J. Biol. Chem.* **283,** 29156–29165
52. Bai, Y., Sivori, D., Woo, S. B., Neet, K. E., Lerner, S. F., and Saragovi, H. U. (2011) During glaucoma, alpha2-macroglobulin accumulates in aqueous humor and binds to nerve growth factor, neutralizing neuroprotection. *Invest. Ophthalmol. Vis. Sci.* **52,** 5260–5265
53. Mantuano, E., Mukandala, G., Li, X., Campana, W. M., and Gonias, S. L. (2008) Molecular dissection of the human alpha2-macroglobulin subunit reveals domains with antagonistic activities in cell signaling. *J. Biol. Chem.* **283,** 19904–19911
54. Gonias, S. L., Carmichael, A., Mettenburg, J. M., Roadcap, D. W., Irvin, W. P., and Webb, D. J. (2000) Identical or overlapping sequences in the primary structure of human $\alpha_2$-macroglobulin are responsible for the binding of nerve growth factor-beta, platelet-derived growth factor-BB, and transforming growth factor-beta. *J. Biol. Chem.* **275,** 5826–5831
55. Shi, Y., Yamauchi, T., Gaultier, A., Takimoto, S., Campana, W. M., and Gonias, S. L. (2011) Regulation of cytokine expression by Schwann cells in response to α2-macroglobulin binding to LRP1. *J. Neurosci. Res.* **89,** 544–551
56. Artym, V. V., Zhang, Y., Seillier-Moiseiwitsch, F., Yamada, K. M., and Mueller, S. C. (2006) Dynamic interactions of cortactin and membrane type 1 matrix metalloproteinase at invadopodia: defining the stages of invadopodia formation and function. *Cancer Res.* **66,** 3034–3043
57. Li, X. Y., Ota, I., Yana, I., Sabeh, F., and Weiss, S. J. (2008) Molecular dissection of the structural machinery underlying the tissue-invasive activity of membrane type-1 matrix metalloproteinase. *Mol. Biol. Cell.* **19,** 3221–3233
58. Remacle, A., Murphy, G., and Roghi, C. (2003) Membrane type I-matrix metalloproteinase (MT1-MMP) is internalised by two different pathways and is recycled to the cell surface. *J. Cell Sci.* **116,** 3905–3916
59. Wang, X., Ma, D., Keski-Oja, J., and Pei, D. (2004) Co-recycling of MT1-MMP and MT3-MMP through the trans-Golgi network. Identification of DKV582 as a recycling signal. *J. Biol. Chem.* **279,** 9331–9336
60. Williams, K. C., and Coppolino, M. G. (2011) Phosphorylation of membrane type 1-matrix metalloproteinase (MT1-MMP) and its vesicle-associated membrane protein 7 (VAMP7)-dependent trafficking facilitate cell invasion and migration. *J. Biol. Chem.* **286,** 43405–43416
61. Ranganathan, S., Liu, C. X., Migliorini, M. M., Von Arnim, C. A., Peltan, I. D., Mikhailenko, I., Hyman, B. T., and Strickland, D. K. (2004) Serine and threonine phosphorylation of the low density lipoprotein receptor-related protein by protein kinase Cα regulates endocytosis and association with adaptor molecules. *J. Biol. Chem.* **279,** 40536–40544
62. Lehti, K., Rose, N. F., Valavaara, S., Weiss, S. J., and Keski-Oja, J. (2009) MT1-MMP promotes vascular smooth muscle dedifferentiation through LRP1 processing. *J. Cell Sci.* **122,** 126–135
63. Wickramasinghe, R. D., Ko Ferrigno, P., and Roghi, C. (2010) Peptide aptamers as new tools to modulate clathrin-mediated internalisation–inhibition of MT1-MMP internalisation. *BMC Cell. Biol.* **11,** 58
64. Trommsdorff, M., Borg, J. P., Margolis, B., and Herz, J. (1998) Interaction of cytosolic adaptor proteins with neuronal apolipoprotein E receptors and the amyloid precursor protein. *J. Biol. Chem.* **273,** 33556–33560
65. Muratoglu, S. C., Mikhailenko, I., Newton, C., Migliorini, M., and Strickland, D. K. (2010) Low-density lipoprotein receptor-related protein 1 (LRP1) forms a signaling complex with platelet-derived growth factor receptor-beta in endosomes and regulates activation of the MAPK pathway. *J. Biol. Chem.* **285,** 14308–14317

*Received for publication October 26, 2012.*
*Accepted for publication April 22, 2013.*